pubs.acs.org/Biomac

Article

PEDOT:PSS in Solution Form Exhibits Strong Potential in Inhibiting SARS-CoV-2 Infection of the Host Cells by Targeting Viruses and Also the Host Cells

Jo-Ning Hung, Di Ngoc Kha Vo, Ha Phan Thanh Ho, and Ming-Han Tsai*

Cite This: https://doi.org/10.1021/acs.biomac.2c00271

Read Online

ACCESS | Metrics & More | Article Recommendations | Supporting Information

ABSTRACT: Severe acute respiratory syndrome coronavirus 2 (SARS-CoV-2) has caused a global pandemic with over 5 million fatalities. Vaccines against this virus have been globally administered; however, SARS-CoV-2 variants with spike protein mutations are continuously identified with strong capability to escape vaccine-elicited protection. Due to the high mutation rate and transmission ability, the development of a broad-spectrum SARS-CoV-2 inhibitor is highly in demand. In this study, the effect of poly(3,4-ethylenedioxythiophene):poly(styrene sulfonate) (PEDOT:PSS) against SARS-CoV-2 was investigated. The treatment of pseudoviruses carrying the SARS-CoV-2 spike protein with PEDOT:PSS strongly blocked SARS-CoV-2 pseudovirus infection in human ACE2-expressing cells without causing cytotoxicity. Specifically, PEDOT:PSS showed great potential in both inactivating viruses and rendering antiviral activity to the treated cells. The effects of other PEDOT:PSS solutions with different chemical ratios and properties were also validated to find the high inhibition capacity against SARS-CoV-2 pseudovirus infection. The transcriptomic data reveal that PEDOT:PSS-treated cells were endowed with transcriptional alteration, and it could be reverted after the removal of PEDOT:PSS from the culture medium. Importantly, PEDOT:PSS also exhibited broad-spectrum inhibition effects on the pseudovirus carrying the spike protein isolated from different variants. In combination with the advantage of high biocompatibility, PEDOT:PSS could thus be considered a potential therapeutic and prophylactic material against SARS-CoV-2.

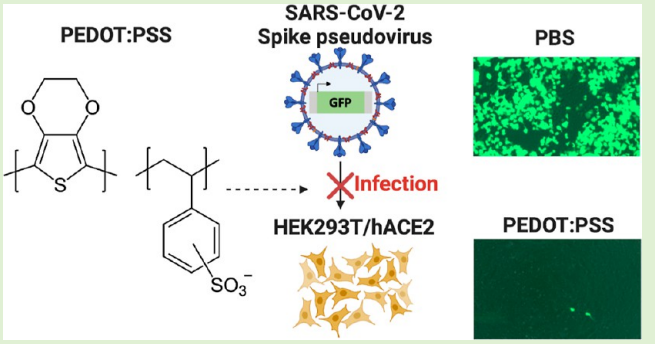

1. INTRODUCTION

COVID-19 is an emerging disease caused by severe acute respiratory syndrome coronavirus 2 (SARS-CoV-2).[1] Since the report of the first case in December 2019, it has rapidly become a pandemic disease with more than 530 million cases and is responsible for over 6 million fatalities.[1] SARS-CoV-2 is an enveloped single-strand positive RNA virus, and its genome length ranges from 26 to 32 kb. With high genetic similarity to SARS-CoV, the SARS-CoV-2 virus utilizes its spike protein for binding and entering the host cells through recognizing the angiotensin-converting enzyme 2 (ACE2) protein expressed on the host cell surface.[2,3] Ultimately, the spike protein is considered the best vaccine candidate since the neutralizing antibodies targeting the spike protein offer prophylactic effects against COVID-19 by blocking the receptor-binding site of SARS-CoV-2 in the host cells. Numerous vaccines have been designed with this principle and currently have been utilized globally to vaccinate against SARS-CoV-2 infection.[4,5] Nevertheless, due to the high mutation rate of RNA viruses as well as the high transmission efficiency of SARS-CoV-2, it is conceivable that the SARS-CoV-2 variants with mutations on the Spike gene could ultimately lead to their immune escape from the neutralizing antibodies that had been acquired after the previous SARS-CoV-2 infection or vaccination of the spike protein derived from the most original SARS-CoV-2 strain.[4,6−10] In parallel, there are numerous viral proteins with immunosurveillance property that could compromise the long-term antiviral effects post-SARS-CoV-2 infection.[11−16] Consequently, it is essential to consider other strategies against SARS-CoV-2 infection besides vaccination, such as antiviral drugs with a broad-spectrum inhibition of SARS-CoV-2 infection. For example, Paxlovid (PF-07321332 plus ritonavir) inhibits viral replication at the proteolysis stage that is required for viral RNA replication.[17,18] In addition, several drugs against viral RNA-dependent RNA polymerase (RdRp) had also been investigated, such as Remdesivir and Molnupiravir, which are nucleoside analogues that can be incorporated by the RdRp

Received: March 1, 2022
Revised: July 18, 2022

into the growing RNA, leading to error in viral protein translation.[19−23] However, all the above drugs are proposed for the inhibition of viral replication after SARS-CoV-2 infection but are not designed for the prevention of viral infection and transmission. Similar to vaccination, the mutations acquired by SARS-CoV-2 during its evolution might also lead to the loss of efficacy of these antiviral drugs since they specifically target viral proteins. On the other hand, while many chemicals can naturally offer strong efficacy in the inactivation of viruses by denaturing the proteins or disrupting the membrane integrity, many of these chemicals are hardly applied in medical usage due to high cell toxicity. Nevertheless, some graphene-based or other carbon-based materials have been implicated in many antimicrobial functions, including the inhibition of SARS-CoV-2 infection, and had been tested in several cell-based experiments.[24−29] Interestingly, the charge-carrying property of these substances is considered as one of the key factors for inhibiting the infection of SARS-CoV-2.[29] However, many of them are currently designed as sheets, coating materials, or nanoparticles, which require specific alterations to addend high efficacy and low cell toxicity properties.[24,29,30] Moreover, certain graphene-based 3D materials might raise concerns causing inflammation in animals.[30−32] Nevertheless, these research works reveal the great potential of graphene-based materials in biomedical applications. Therefore, advanced modifications or other forms of such materials deserve to be further inspected.

In this study, we investigated whether the highly conductive polymer material poly(3,4-ethylenedioxythiophene):poly(styrene sulfonate) (PEDOT:PSS) offers the ability to inhibit SARS-CoV-2 infection in a cell-based model. PEDOT:PSS is a conductive macromolecular material, in which PEDOT is a conjugated polymer carrying positive charges, whereas sulfonyl groups of PSS offer negative charges. PEDOT:PSS has been applied in many biomedical devices and bio-conductive applications due to its conductivity, and most importantly its favorable cytocompatibility.[33−39] Interestingly, PEDOT:PSS had been previously reported to have a potential function in blocking bacterial growth, which also implies its possibility to be applied in fighting against microorganisms.[40] However, the usage of PEDOT:PSS is mostly based on coated films, microballs, hydrogels, or other formats, while the usage of PEDOT:PSS in the aqueous form had not been fully investigated.[33,41−44] Here, we showed that PEDOT:PSS in an aqueous solution exhibits extremely low cytotoxicity to the treated cells. Meanwhile, we also demonstrated that the addition of PEDOT:PSS, even at low concentrations, can readily cause such an extraordinary inhibition of the SARS-CoV-2 pseudovirus in cells that overexpress human ACE2. Mechanically, PEDOT:PSS not only shows strong inactivation effects on SARS-CoV-2 pseudoviruses but also allows the cells exposed to PEDOT:PSS just for a shorter period to exhibit resistance effects against SARS-CoV-2 pseudovirus infection. The inhibition properties of several PEDOT:PSS solution formulas against SARS-CoV-2 infection were also validated, and significant inhibition effects were observed, although to different extents, depending on different formulas. Importantly, PEDOT:PSS treatment can also influence the transcriptomic patterns of the cells, and these changes can be reversed after the removal of PEDOT:PSS from the culture medium. Ultimately, the inhibition effects of PEDOT:PSS aqueous solution against SARS-CoV-2 pseudoviruses with different spike protein mutations were also examined. Our work highlights that PEDOT:PSS aqueous solution could be considered as a potential antiviral material owing to its huge capacity in medical usage for human body with extremely low cytotoxicity.

2. EXPERIMENTAL SECTION

2.1. Cell Lines and Cell Culture. HEK293T cells are derived from human embryonic kidney cells that contain the SV40 T-antigen (ATCC: CRL-3216). HEK293T cells stably expressing human ACE2 (HEK293T/hACE2) were obtained after transduction with lentiviruses carrying hACE2 and blasticidin resistance gene and were treated with blasticidin (10 μg mL^{-1}). All cells used in this study were maintained in RPMI medium (Invitrogen) supplemented with 10% fetal calf serum (FBS, HyClone) in a humidified cell culture incubator at 37 °C.

2.2. Transfection. All transfection experiments were performed with PEI MAX (MW: 40,000, Polysciences 24765-1) following the manufacturer's instructions.

2.3. Cell Viability. 3×10^3 HEK293/hACE2 cells per well were seeded in a 96-well culture plate and incubated overnight. Cells were treated with PEDOT:PSS aqueous solution with the indicated dilutions in the culture medium for 24−48 h. After incubation, cell viability was evaluated by the MTT assay.

2.4. PEDOT:PSS. PEDOT:PSS aqueous solution (with a 1:6 ratio of PEDOT to PSS and 1.3−1.7% solid content in water, Clevios AI4083, Heraeus Electronic Materials) was applied for all experiments in this study except for the study given in Section 2.3 where the PEDOT:PSS aqueous solution made with different formulas (provided by DAILY POLYMER Corporation, Taiwan) was utilized.

2.5. Plasmids and Oligonucleotides. pLAS2 is a lentiviral vector with the CMV promoter and was obtained from the RNAi Core, Academia Sinica, Taiwan. We, therefore, inserted a GFP gene after the CMV promoter of the pLAS2 lentiviral plasmid (pLAS2-GFP). A plasmid encoding the SARS-CoV-2 Spike gene with D614G + N501Y mutations (D614G/N501Y) with a cytoplasmic tail deletion of 13 amino acids (pcDNA3.1-Spike D614G/N501Y delCT13) kindly provided by the RNAi Core, Academia Sinica, Taiwan, was used for the generation of Spike pseudovirus for most of this study besides Section 3.6.

The following plasmids were constructed for the generation of Spike pseudoviruses carrying the spike protein with different mutations. pcDNA3.1-SARS2-Spike is an expression plasmid carrying the wild-type SARS-CoV-2 spike protein with a C9 tag at its terminus and was a gift from Fang Li (Addgene plasmid #145032). Expression plasmids carrying important spike protein clinical variants, namely, pcDNA3.1-SARS2-Spike with D614G or D614G + N501Y mutations, were generated using pcDNA3.1-SARS2-Spike (Addgene plasmid #145032) as the backbone and modified by polymerase chain reaction (PCR) cloning. Expression plasmid carrying the spike protein D614G + N501Y was applied for most of the transfection and pseudovirus production experiments, and a few exceptions were carefully annotated. A series of spike mutations or deletions were constructed using pcDNA3.1-SARS2-Spike D614G/N501Y and overlapping PCR, which include L18F/T20N/P26S, T19R, and the deletion mutations HV 69-70. Expression plasmids carrying the spike protein derived from Delta strain (pTwist-SARS-CoV-2 Δ18 B.1.617.2V1, Addgene plasmid #179905) or Omicron strain (pTwist-SARS-CoV-2 Δ18 B.1.1.529, Addgene plasmid #179907) were gifts from AleJandro Balazs.[45] The sequences of the plasmids were further validated through Sanger sequencing. The lenti-ACE2 plasmid and a synthesized codon-optimized Spike gene constructed in pcDNA3.1 were gifts from Academia Sinica, Taiwan. All synthesized oligonucleotides are listed in Supporting Information Table S1.

2.6. Production of Pseudovirions and Cell Transduction. Pseudovirions were produced by the co-transfection of HEK293T cells with pCMVR8.91, pLAS2-GFP lentiviral plasmids, and plasmids encoding different SARS-CoV-2 Spike genes at the ratio of 6.25:6.5:1.1 using PEI transfection. For the majority of the experiment, a plasmid encoding SARS-CoV-2 Spike gene

https://doi.org/10.1021/acs.biomac.2c00271
Biomacromolecules XXXX, XXX, XXX−XXX

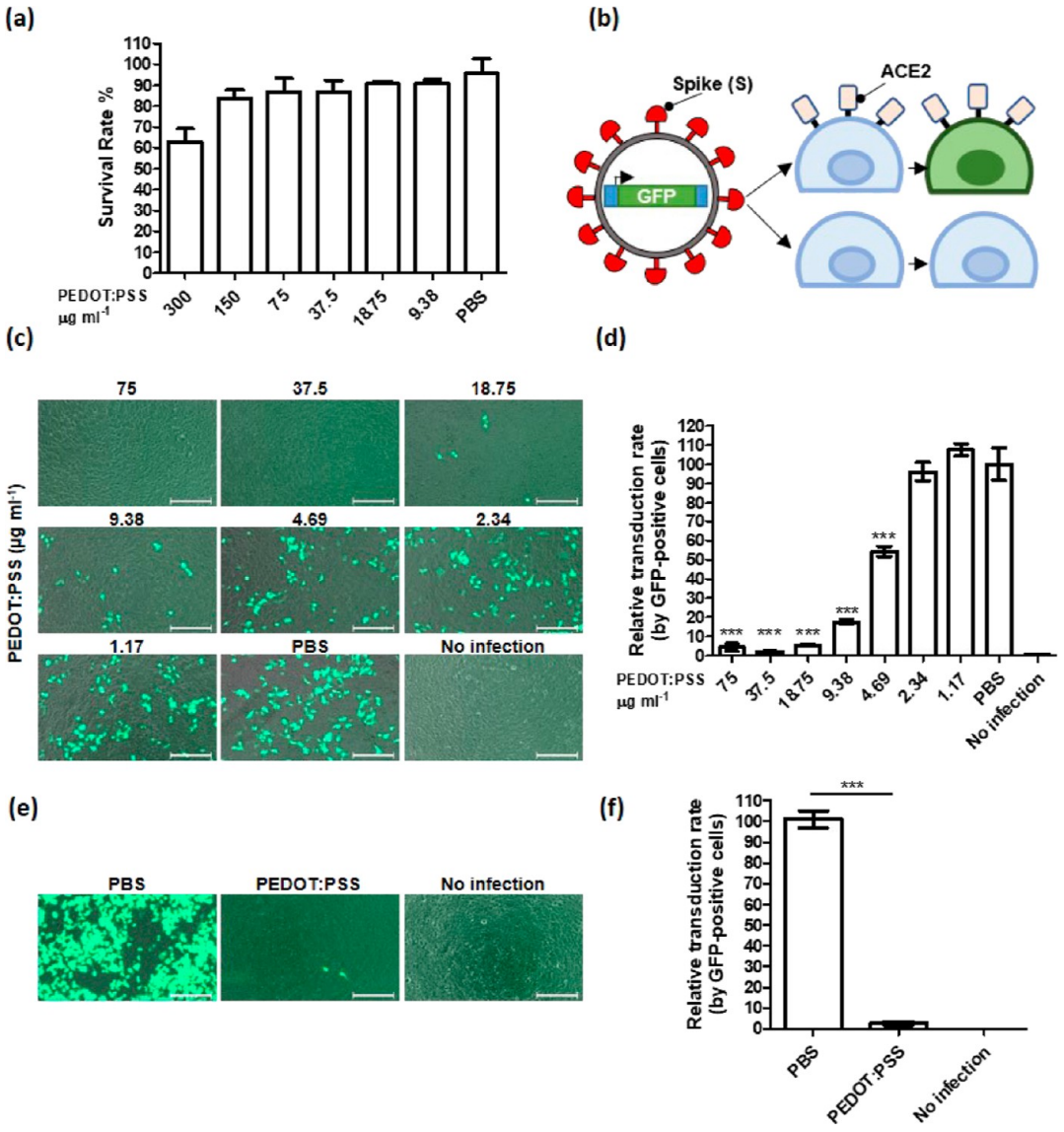

Figure 1. PEDOT:PSS did not inhibit cell viability but can efficiently reduce SARS-CoV-2 Spike pseudovirus infection in a dose-dependent manner. (a) HEK293T/hACE2 cells were treated with various dilutions of PEDOT:PSS for 48 h, and the viability of the treated cells was evaluated by the MTT assay. (b) Scheme of Spike pseudovirus carrying GFP in its viral genome. (c,d) HEK293T/hACE2 cells were treated with different dilutions of PEDOT:PSS in the culture medium and infected with Spike pseudovirus for 48 h. The infected cells were GFP-positive that can be (c) visualized by fluorescence microscopy or (d) quantified by flow cytometry. (e,f) In one experiment, the 10-fold concentration of Spike pseudovirus was used for infecting HEK293T/hACE2 cells by treatment with PEDOT:PSS at 75 μg mL^{-1} concentration. The infectivity of these cells was evaluated 48 h post-infection by (e) fluorescence microscopy and (f) flow cytometry. The data are shown as means ± SDs (error bars). Student's *t*-test was used, and $P < 0.05$ indicates a statistically significant difference; ***$P < 0.001$. The scale bar in the figures represents 100 μm.

(pcDNA3.1-Spike D614G/N501Y delCT13) was used for the generation of Spike pseudovirus, whereas the other plasmids encoding Spike genes with further mutations were applied while generating the Spike pseudoviruses containing the spike protein with the desired mutations. In some experiments, the pseudovirus carrying vesicular stomatitis virus G glycoprotein (VSV-G) was achieved by using the same protocol of generating Spike pseudovirus, but the spike-expressing plasmid was replaced with a plasmid encoding VSV-G. The supernatants were collected 60 h post-transfection and passed through 0.45 μm filters. To evaluate the transduction efficiency of each pseudoviral sample, 5000 HEK293T/hACE2 cells were seeded in 96-well plates per well and inoculated with the supernatants containing Spike pseudovirions. The transduction efficiency of each pseudoviral sample was evaluated 48 h post-transduction by detecting the percentage of GFP-positive cells, which was visualized using a fluorescence microscope (Zeiss) or quantified by flow cytometry (FACSCalibur).

2.7. Spike Pseudovirion Purification. The SARS-CoV-2 Spike pseudovirions from the supernatant can be further concentrated by pelleting down the viral particles through the sucrose centrifugation method. In brief, the virus-containing supernatant was overlaid on a sucrose-containing buffer (50 mM Tris−HCl, pH 7.4, 100 mM NaCl, 0.5 mM ethylenediaminetetraacetic acid) at a 4:1 v/v ratio and centrifuged at 10,000×*g* at 4 °C for 4 h. After centrifugation, the supernatant was carefully removed, and the pellets containing viruses were collected by resuspending in PBS.

2.8. Viral Binding Assay. The pseudovirus samples with or without pre-treatment of PEDOT:PSS were incubated with 20,000 HEK293T/hACE2 cells under constant rolling at 4 °C. After 1 h of incubation, the cells were collected by centrifugation, washed with PBS, and dropped on glass slides. The cell-bound SARS-CoV-2 Spike pseudovirions were first recognized by the rabbit polyclonal antibody against the spike protein and therefore were visualized by using the Cy-3 conjugated antibody. In some experiments, we quantified the

https://doi.org/10.1021/acs.biomac.2c00271
Biomacromolecules XXXX, XXX, XXX−XXX

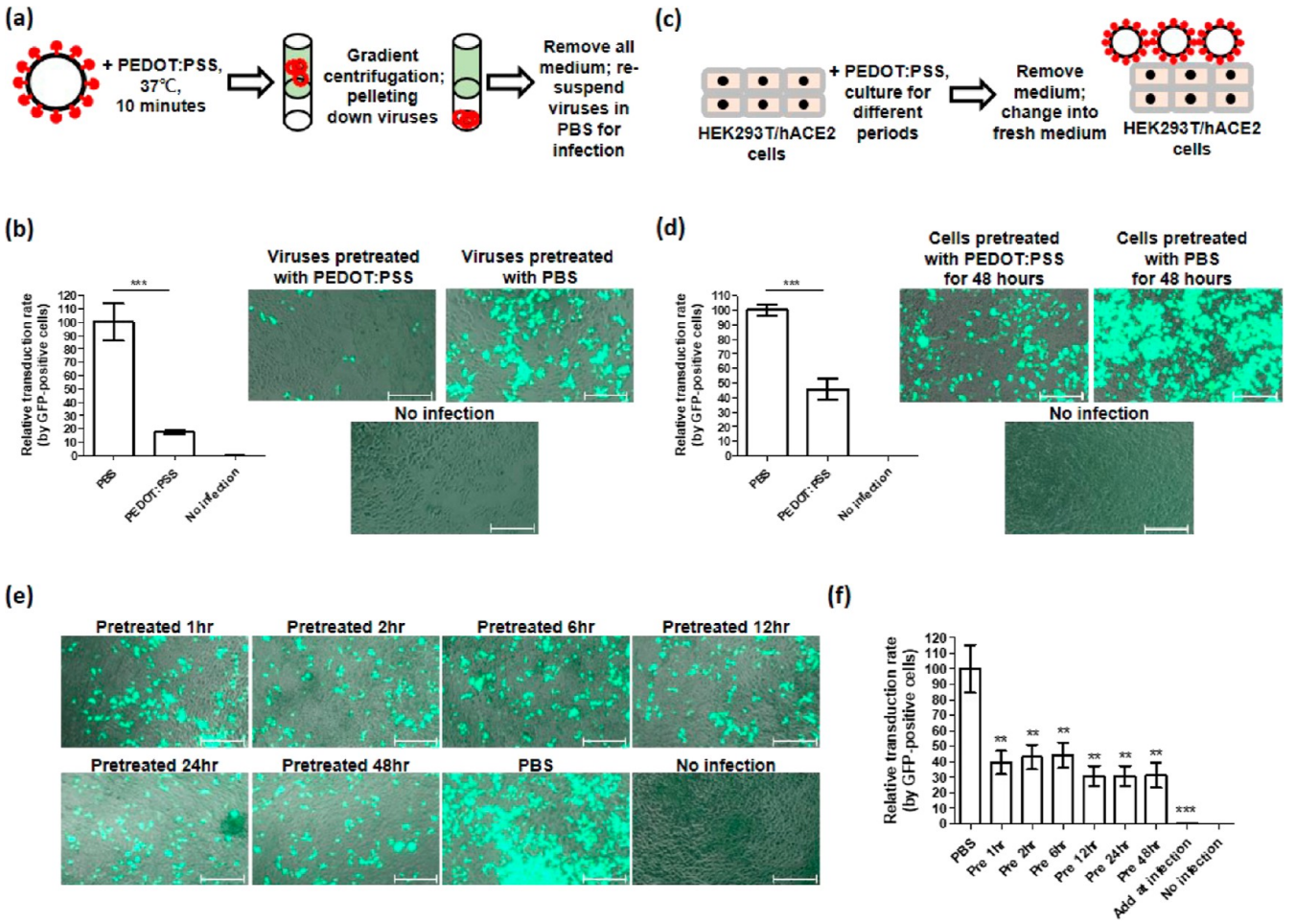

Figure 2. PEDOT:PSS inhibits Spike pseudovirus infection of HEK293T/hACE2 cells by targeting both viruses and cells. (a) Schematic design of PEDOT:PSS pre-treatment to the viruses. Here, 75 μg mL^{-1} PEDOT:PSS was added to the supernatant containing Spike pseudoviruses for 10 min at 37 °C. The PEDOT:PSS-treated viral particles can be pelleted down through a sucrose gradient centrifugation that allows the removal of PEDOT:PSS from the supernatants. (b) HEK293T/hACE2 cells were treated with Spike pseudoviruses that had been pretreated with 75 μg mL^{-1} PEDOT:PSS or PBS. The percentage of infected cells showing the GFP-positive signal was evaluated by both flow cytometry and fluorescence microscopy. (c) Schematic design of PEDOT:PSS pre-treatment to the cells. Here, 75 μg mL^{-1} PEDOT:PSS was added to the cell supernatant. After incubating with PEDOT:PSS for the indicated periods, the culture supernatant containing PEDOT:PSS was entirely removed and replaced with a fresh culture medium. (d) HEK293T/hACE2 cells were first treated with 75 μg mL^{-1} PEDOT:PSS for 48 h. The culture medium was then entirely removed and replaced with a fresh medium containing Spike pseudoviruses. The percentage of infected cells showing the GFP-positive signal was evaluated by flow cytometry and fluorescence microscopy 48 h post-infection. (e,f) Similar experiment as (d) but with different periods of PEDOT:PSS pre-treatment. In (f), an extra group "Add at infection" represents the cells treated with PEDOT:PSS at the time of virus infection and incubated for 48 h without replenishing the medium. The data are shown as means ± SDs (error bars). Student's *t*-test was used, and $P < 0.05$ indicates a statistically significant difference; $^{**}P < 0.01$, $^{***}P < 0.001$. The scale bar in the figures represents 100 μm.

amount of the bound viral particles by using flow cytometry. Here, the viral-bound cells were also stained with the rabbit polyclonal antibody and stained with the secondary antibody conjugated with PE. The stained cells were subjected to flow cytometry (FACSCalibur). The data were further analyzed using FlowJo software.

2.9. RNA Extraction and Reverse Transcription-Quantitative PCR of the Purified Viruses. Total RNA was extracted from cell lines using a GENEzol TriRNA Pure Kit (Geneaid) according to the manufacturer's instructions. Total RNA was dissolved in 40 μL of RNase-free water, 10 μL of which was reverse-transcribed into cDNA using random hexamers and a RevertAid First Strand cDNA Synthesis Kit (Thermo Scientific, USA). All RNA samples without the treatment of reverse transcriptase served as negative controls. Reverse transcription-quantitative PCR (RT-qPCR) was performed with the ABI StepOnePlus system according to the SYBR Green method. Cycle threshold (CT) values were determined using fixed threshold settings after completion of the reaction. The relative quantity of cDNA-containing GFP sequence in each sample was shown as CT values. Primer sequences are listed in Supporting Information Table S1.

2.10. RNA Sequencing and Bioinformatics Analyses. Samples including HEK293T/hACE2 cells pretreated with PEDOT:PSS at 200-fold dilution (75 μg mL^{-1}) for 24 h, HEK293T/hACE2 cells pretreated under similar conditions with an additional day for recovery after the removal of PEDOT:PSS, and HEK293T/hACE2 cells treated with PBS only as the control were collected for RNA extraction and subjected to RNA sequencing.

The purified RNA was used for the preparation of the sequencing library using the TruSeq Stranded mRNA Library Prep Kit (Illumina, San Diego, CA, USA) following the manufacturer's recommendations. Briefly, mRNA was purified from total RNA (1 μg) by oligo(dT)-coupled magnetic beads and fragmented into small pieces at elevated temperature. The first-strand cDNA was synthesized using reverse transcriptase and random primers. After the generation of double-strand cDNA and adenylation on 3′ ends of DNA fragments, the adaptors were ligated and purified with an AMPure XP system

https://doi.org/10.1021/acs.biomac.2c00271
Biomacromolecules XXXX, XXX, XXX−XXX

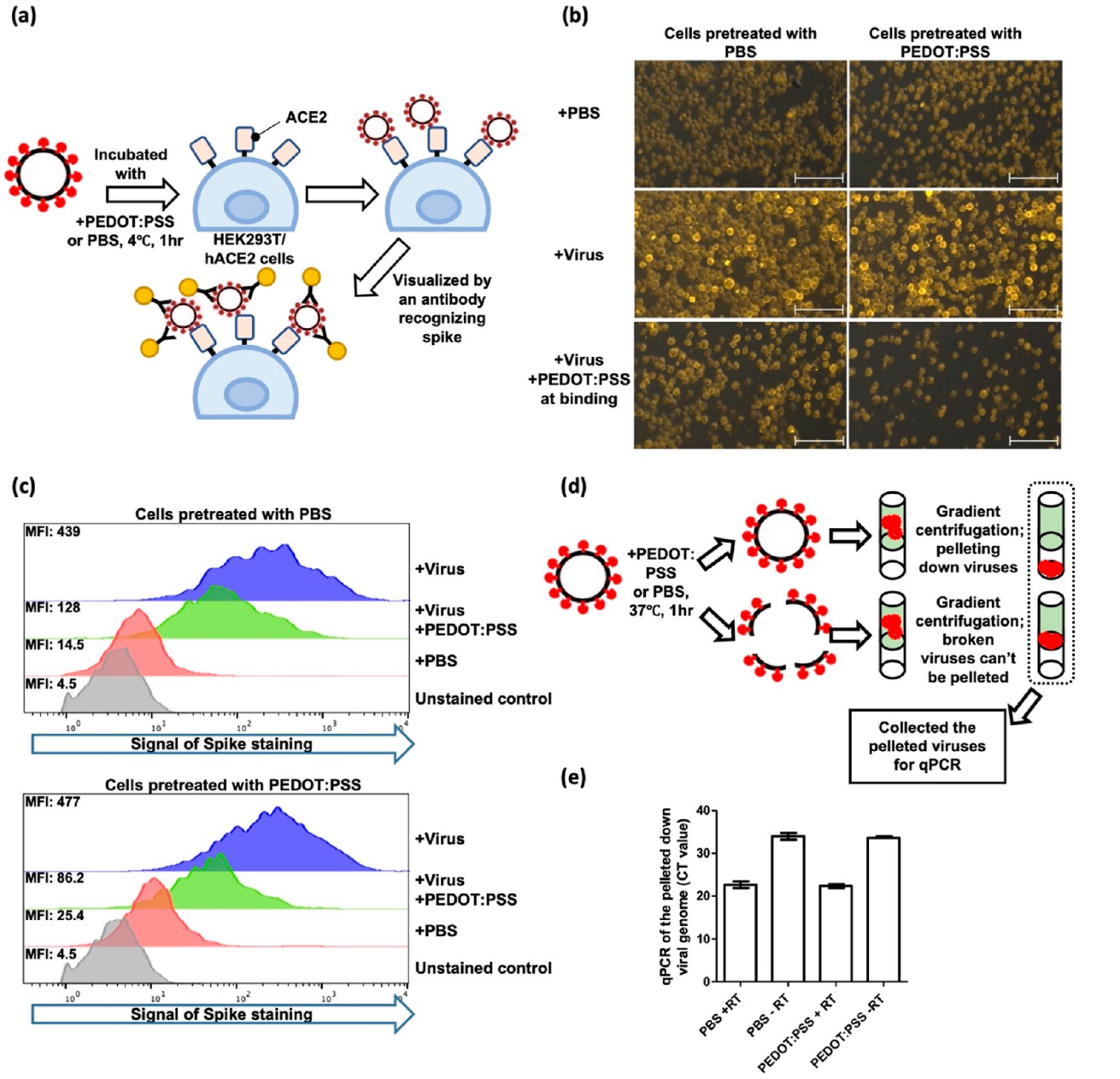

Figure 3. PEDOT:PSS inhibits the Spike pseudoviruses from binding to HEK293T/hACE2 cells. (a) Schematic design of the binding assay. (b,c) HEK293T/hACE2 cells were pretreated with 75 μg mL^{-1} PEDOT:PSS (or PBS) for 1 h at 37 °C, followed by two times of washing to entirely remove PEDOT:PSS. Next, the binding assay was performed for 1 h at 4 °C with or without adding PEDOT:PSS during binding by using both Spike pseudoviruses and the pretreated cells. Finally, the Spike pseudoviruses bound to HEK293T/hACE2 cells were visualized through (b) an immunofluorescence staining assay by using the antibody specific to the spike protein and further labeled with the Cy3-conjugated secondary antibody or (c) flow cytometry by using the PE-conjugated secondary antibody. MFI: mean fluorescence intensity. Negative control: cells without staining with antibodies. (d) Schematic design of a procedure validating the virus recovery efficiency after pre-treatment and gradient centrifugation. The Spike pseudoviruses were pretreated with 75 μg mL^{-1} PEDOT:PSS or PBS for 1 h at 37 °C. Next, gradient centrifugation was performed to collect virus pellets and remove the supernatant containing PEDOT:PSS. Ultimately, only intact virus particles can pass through the sucrose cushion and be pelleted down. (e) Virus pellets collected from (d) were hereby extracted and subjected to RT-qPCR to quantify the amount of viral genome by using the primers specific to the GFP sequence of the pseudovirus. +RT: with reverse transcription; −RT: without adding reverse transcriptase as the control. The scale bar in the figures represents 100 μm.

(Beckman Coulter, Beverly, USA). The quality of the libraries was assessed on the Agilent Bioanalyzer 2100 system and a real-time PCR system. The qualified libraries were then sequenced on an Illumina NovaSeq 6000 platform with 150 bp paired-end reads generated by Genomics, BioSci & Tech Co., New Taipei City, Taiwan.

After getting sequencing reads, the bases with low quality and sequences from adapters in raw data were removed using the Trimmomatic program (version 0.39).[46] The filtered reads were aligned with the reference genomes GRCh37 using Bowtie2 (version 2.3.4.1).[47] The RSEM software (version 1.2.28) was applied for the quantification of the transcript abundance.[48] The transcriptional level of each gene was further converted into FPKM (fragments per kilobase of transcript per million mapped reads) and applied for analyses. Here, the transcriptional heatmap comparing the indicated transcription of the selected genes was created by using Heatmapper

https://doi.org/10.1021/acs.biomac.2c00271
Biomacromolecules XXXX, XXX, XXX−XXX

software,[49] and pathway analyses were done by using Ingenuity Pathway Analysis (IPA) software (GIAGEN, Hilden, Germany).

2.11. Statistical Analysis and Software. The differences between two studied groups were analyzed by Student's *t*-tests using the GraphPad Prism 5 software; $p < 0.05$ indicates a statistical difference. The flow cytometry data were evaluated using FlowJo software. The table of content (ToC) graph was created with BioRender.com with license.

3. RESULTS

3.1. PEDOT:PSS Solution Shows Strong Inhibition Capacity against SARS-CoV-2 Pseudovirus Infection in Cells with Human ACE2 Overexpression without Significant Cytotoxicity. To examine the efficacy and potential mechanisms of PEDOT:PSS in the prevention of SARS-CoV-2 infection, the HEK293T cells stably expressing human ACE2 protein (HEK293T/hACE2) were generated. The PEDOT:PSS solution examined here was acquired from Heraeus Clevious AI 4083, in which the PEDOT:PSS ratio is 1:6. Through the MTT assay, we found that except at high concentrations (300 μg mL^{-1}), PEDOT:PSS solution did not significantly inhibit the cell viability of HEK293T/ACE2 in 24 to 48 h post-treatment (Figure 1a).

Next, we wished to test whether PEDOT:PSS solution could influence SARS-CoV-2 infection. Here, the lentiviral-based pseudotype virus bearing the SARS-CoV-2 spike protein on its viral envelope and carrying a CMV-promoter driven GFP gene in its viral genome was generated (termed Spike pseudovirus) for the evaluation of the effects of PEDOT:PSS on SARS-CoV-2 infection (Figure 1b). Based on this design, the cells successfully infected by this Spike pseudovirus were GFP-positive, and the infectivity can be visualized by a fluorescence microscope or quantified by flow cytometry. Importantly, as evidence for successful simulation of the live SARS-CoV-2 virus, this Spike pseudovirus shows high specificity to ACE2-positive cells, while it barely infects the cells without ACE2 overexpression (Supporting Information Figure S1). By adding PEDOT:PSS at the indicated dilution during infection, our data showed that PEDOT:PSS had strong ability to inhibit SARS-CoV-2 pseudovirus infection of HEK293T/hACE2 in a dose-dependent manner by greatly reducing the GFP-positive cells after infection (Figure 1c,d). Surprisingly, we barely observed any infected cells when the dilution of PEDOT:PSS was lower than 37.5 μg mL^{-1}, and the corresponding inhibition rate detected by flow cytometry could reach nearly 100%. These exceptional inhibition effects can also be achieved even when using a higher amount of Spike pseudovirus (Figure 1e). Taken together, these findings suggested that PEDOT:PSS in solution form might act as a superlative candidate for inhibiting SARS-CoV-2 infection.

3.2. PEDOT:PSS Inhibits SARS-CoV-2 Pseudovirus Infection of Targeted Cells by Inactivating the Virus and Endowing the Treated Cells with Antiviral Potential. In order to investigate how PEDOT:PSS inhibited Spike pseudovirus infection in the HEK293/hACE2 cell culture system, infectivity tests were performed to determine whether PEDOT:PSS in solution could directly inactivate the Spike pseudoviruses. Viral supernatants were first treated with PEDOT:PSS at 75 μg mL^{-1} for 10 min at 37 °C. Subsequently, the viral particles were pelleted down by gradient centrifugation to entirely remove the supernatant containing PEDOT:PSS. The pelleted-down viruses were further resuspended in PBS and applied for infectivity tests. The whole procedure is graphically depicted in Figure 2a. The results showed that the Spike pseudoviruses pretreated with PEDOT:PSS for 10 min at 37 °C lost 80% of infectivity compared with the viruses pretreated with PBS only (Figure 2b). Moreover, whether the PEDOT:PSS pretreated cells could gain higher antiviral activity against SARS-CoV-2 infection should also be considered. Here, HEK293T/hACE2 cells were pretreated with 75 μg mL^{-1} PEDOT:PSS for 48 h. Subsequently, the culture medium was entirely removed and replaced with a fresh medium containing Spike pseudovirus (Figure 2c). Our result revealed that cells pretreated with PEDOT:PSS for 48 h showed more than 50% reduction in infection rate in comparison with the cells pretreated with PBS only (Figure 2d). This result was further investigated by comparing the Spike pseudovirus infectivity of HEK293T/hACE2 cells pretreated with PEDOT:PSS for different periods. Surprisingly, we observed that the HEK293T/hACE2 cells pretreated with PEDOT:PSS for merely 1 h can readily resist half of the Spike pseudovirus infection (Figure 2e,f). Taken together, these results indicated that PEDOT:PSS could efficiently block Spike pseudovirus infection through inactivating the viral particles even with only a short period of treatment as well as endowing the treated cells with the ability to resist SARS-CoV-2 infection.

3.3. PEDOT:PSS Impedes the Binding of the Spike Pseudovirus to the ACE2-Expressing Cells. We had confirmed that Spike pseudovirus pre-treated with PEDOT:PSS showed strong inhibition against Spike pseudovirus infection in ACE2-expressing cells. To further investigate this mechanism, a viral binding assay was performed to visualize the Spike pseudoviruses bound to the HEK293T/hACE2 cells through immunofluorescence staining (Figure 3a). Here, the cells were pretreated with PEDOT:PSS or PBS for 1 h and then subjected to the binding assay. The result showed that the pre-treatment of cells with PEDOT:PSS had minor effects on viral binding, whereas treatment of PEDOT:PSS during viral binding had strong effects on reducing the Spike pseudovirions bound to HEK293T/hACE2 cells (Figure 3b,c). In addition, to confirm that the reduction of viral infection and binding activity were not due to the disruption of viruses, which could lead to insufficient viral sedimentation, we performed RNA extraction for the pelleted-down viruses, and samples were subjected to RT-qPCR to quantify the amount of the viral genome in each sample. The qPCR analysis showed that PEDOT:PSS-pretreated Spike pseudoviruses still can be efficiently pelleted down using centrifugation through a sucrose cushion without any significant difference in the virus titer compared to the untreated sample (Figure 3d,e). PEDOT:PSS seems to function as the neutralizing factors that could block the interaction between the spike protein and the ACE2 protein, but it does not directly destroy the viral particles since these Spike pseudoviruses are still intact and can be pelleted down through a sucrose cushion. This result suggested that PEDOT:PSS could block the Spike pseudovirus from binding to ACE2-expressing cells *via* shading the interaction between the spike protein and the ACE2 protein but not due to the disruption of viral particles.

3.4. Evaluation of Anti-SARS-CoV-2 Effects of PEDOT:PSS Solutions Composited with Different Chemical Properties. PEDOT:PSS is a charged polymer that can be formulated with different PEDOT-to-PSS-ratios. Its conductivity could also be altered by using different strategies for polymerization. To determine whether PEDOT:PSS

https://doi.org/10.1021/acs.biomac.2c00271
Biomacromolecules XXXX, XXX, XXX−XXX

solutions in different formulas could also have the potential to resist SARS-CoV-2 infection, we here collected five other PEDOT:PSS solutions with different PEDOT-to-PSS ratios as well as different surface resistances measured after forming films. The whole list is shown in Table 1.

Table 1. Information of Different PEDOT:PSS Solutions Examined in This Study

solution	original[a]	1	2	3	4	5
PEDOT-to-PSS ratio	1:6	1:5	1:2.5	1:1.5	1:2.5	1:1.6
resistivity (Ω square)	$5*10^6$ to $-5*10^7$	10^7	10^7	10^7	10^2	10^2

[a]*The PEDOT:PSS solution from Clevios AI4083, Heraeus Electronic Materials were used for the rest of our study.

The cytotoxicity of these PEDOT:PSS solutions was evaluated by the MTT assay 24 h post-treatment, as shown in Figure 4a. To evaluate their effects on the reduction of SARS-CoV-2 infection, equal amounts of Spike pseudoviruses were added to HEK293T/hACE2, and cells were treated with the indicated PEDOT:PSS solution at 75 μg mL^{-1} in the culture medium. The infectivity rate was evaluated by the percentage of GFP-positive cells 48 h post-infection. Interestingly, we found that these PEDOT:PSS solutions with different formulas all showed potential to prevent HEK293T/hACE2 cells from being infected by Spike pseudovirus to different degrees (Figure 4b,c). Strikingly, we also tested the effects of PEDOT:PSS solutions on inhibiting the infection of the same pseudoviruses but composed of glycoproteins derived from another enveloped virus, vesicular stomatitis virus (VSV-G), commonly applied for lentivirus production. However, only 40−60% of reduction in infectivity rate could be observed (Figure 4d,e). To further evaluate their anti-SARS-CoV-2 effects, the Spike pseudoviruses were pretreated with different PEDOT:PSS solutions at 1 to 200 dilutions (approximately 75 μg mL^{-1})for 10 min at 37 °C and were applied for similar experiments described in Figure 2a,b. Our results showed that these PEDOT:PSS solutions all had the ability to inactivate the Spike pseudoviruses, although to a different extent depending on their formulas (Figure 4f,g). In summary, our results revealed that PEDOT:PSS solution has a strong capability for inhibiting SARS-CoV-2 infection, regardless of the PEDOT-to-PSS-ratios as well as their structures post-polymerization.

3.5. Transcriptomic Alteration of the Cells Treated with PEDOT:PSS. We wished to understand how PEDOT:PSS solution endowed the pretreated cells with anti-SARS-CoV-2 ability as described in Figure 2c−e. To achieve this aim, the total RNA was extracted from HEK293T/hACE2 cells treated with PEDOT:PSS for 24 h (PEDOT:PSS-treated group) or treated with PEDOT:PSS in the culture medium for 24 h and subsequently replenished by using the fresh medium for further 24 h (recovered), or the cells pretreated with PBS as the control. Samples were then subjected to RNA-sequence for transcriptome analysis. A heatmap generated by using the transcriptomic data collected from the above groups collected from two independent experiments showed that the cells pretreated with PEDOT:PSS for 24 h had a distinct transcriptomic pattern in comparison to the untreated and also the pretreated then removed groups (Figure 5a). This result showed that PEDOT:PSS indeed has the ability to alter the cells at the transcriptional level, which might be required for the ability to inhibiting SARS-CoV-2 infection. However, the transcriptome reversion of the PEDOT:PSS-treated cells after the removal of PEDOT:PSS for 24 h also indicated that the alteration of transcriptional changes caused by PEDOT:PSS is transient and could be reverted after the removal of PEDOT:PSS. To elucidate the effects of PEDOT:PSS on the treated cells, the gene ontology analysis was performed by using IPA software. Our data showed that PEDOT:PSS could have the potential for inhibiting or activating several pathways (Figure 5b). Interestingly, the treatment of PEDOT:PSS has strong effects on inhibiting the pulmonary fibrosis idiopathic pathway that is aligned with the inhibitory effects of SARS-CoV-2 pathogenesis. Ultimately, we compared the RNA-sequencing data of each gene in between each group from two independent experiments. The whole list of gene candidates with a significant increase or decrease of RNA level post-PEDOT:PSS treatment is shown in Supporting Information Table S2. In conclusion, this study shows the potential of PEDOT:PSS in alternating cellular RNA transcriptome transiently, whereas its detailed mechanism still requires further investigation.

3.6. Broad-Spectrum Antiviral Ability of PEDOT:PSS against the SARS-CoV-2 Pseudoviruses Bearing the Spike Protein with Mutations. We therefore asked whether PEDOT:PSS with broad-spectrum activity against SARS-CoV-2 also has effects against SARS-CoV-2 carrying different kinds of spike protein variants. To achieve this aim, the lenti-based pseudoviruses were packaged by using the spike protein with key mutations that could increase the viral infectivity as previously reported.[50,51] Our results showed that PEDOT:PSS inhibited the infection of all the tested pseudoviruses packaged with different spike mutations (Figure 6a,b). Meanwhile, similar experiments had also been conducted on Spike pseudoviruses comprising the currently pandemic causing Delta and Omicron strains (Supporting Information Figure S2).

4. DISCUSSION

The development of drugs or substances against SARS-CoV-2 infection is important since clinical data revealed that the severity of COVID-19 is positively associated with the detected viral load in those patients.[52,53] Importantly, a broad-spectrum anti-SARS-CoV-2 drug is urgently required since accumulating evidence shows that the emerging SARS-CoV-2 variants have already obtained the ability to escape from the acquired immune memory after vaccination or recovery from a previous viral infection.[50,51,54−56] Thus, PEDOT:PSS has high biocompatibility, low cytotoxicity, and excellent anti-SARS-CoV-2 ability, which could shape this material as the high potential candidate for combating this pandemic disease.

There are several advanced materials that have implicated the functionality against SARS-CoV-2 infection, many of which having great applications in protective clothing materials.[57] Nevertheless, it is inevitable to satisfy the criteria of cytotoxicity if the usage in cells is considered. Graphene or carbon-based materials have been implicated in many antimicrobial functions.[24−28] Besides the wide usage in protective equipment, such as masks,[25] graphene sheets with long alkyl chains inhibit coronavirus replication in cell culture by rupturing SARS-CoV-2 and destructing the virus particles.[24] Through this study, graphene platforms with PGS and alkyl amines of different chain lengths to the surface of graphene

https://doi.org/10.1021/acs.biomac.2c00271
Biomacromolecules XXXX, XXX, XXX−XXX

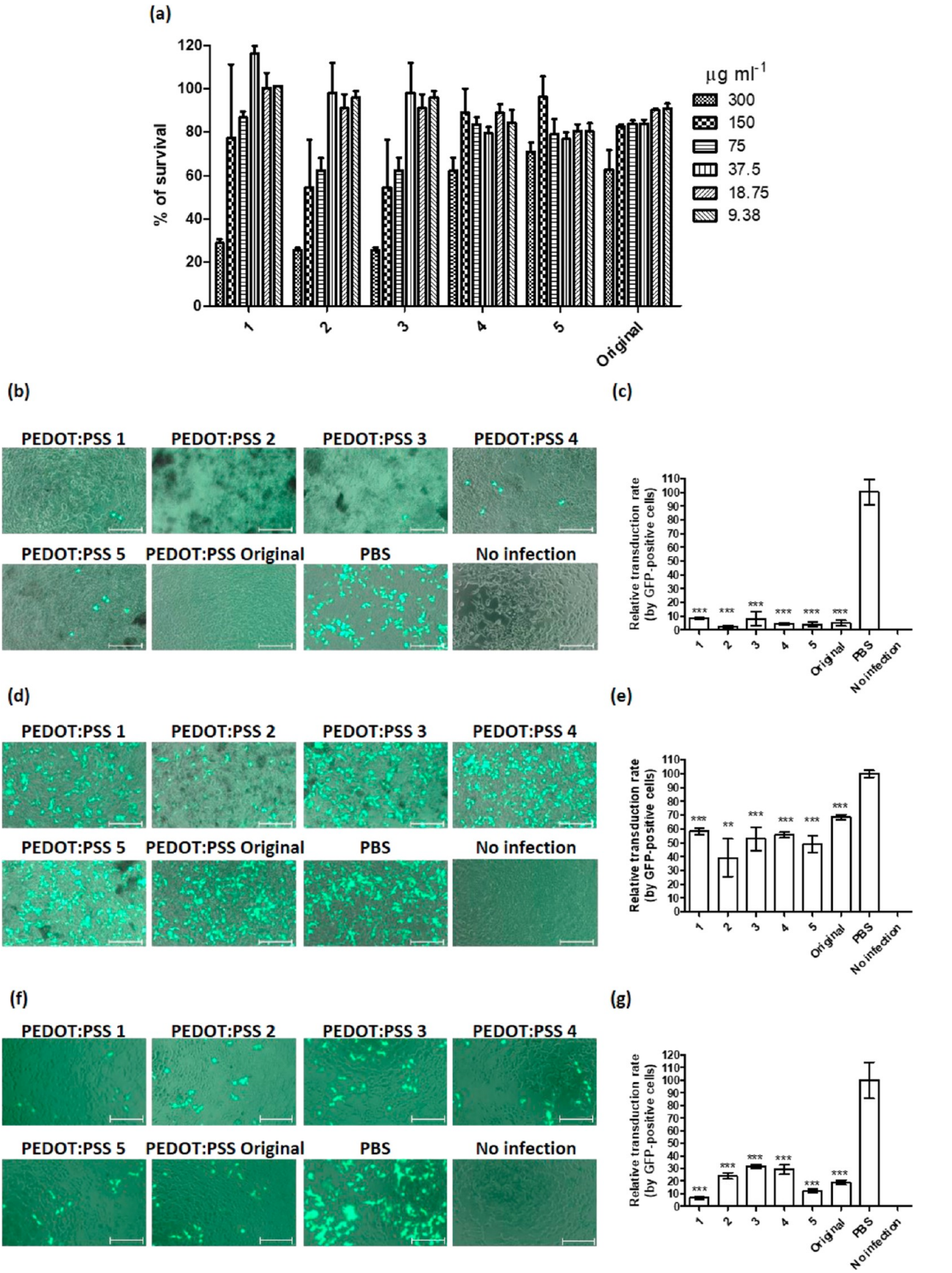

Figure 4. Inhibitory effects against SARS-CoV-2 infection of PEDOT:PSS aqueous solutions made with different formulas. (a) HEK293T/hACE2 cells were treated with different PEDOT:PSS solutions listed in Table 1 for 48 h, and the cell survival rate was evaluated by using the MTT assay. (b−e) HEK293T/hACE2 cells were infected with the (b,c) Spike pseudovirus or (d,e) VSV-G pseudovirus under treatment of the indicated

https://doi.org/10.1021/acs.biomac.2c00271
Biomacromolecules XXXX, XXX, XXX−XXX

Figure 4. continued

PEDOT:PSS solutions at 75 μg mL^{-1}or PBS only. The infectivity was (b,d) visualized by the fluorescence microscope and (c,e) quantified by flow cytometry. (f,g) Spike pseudoviruses were pretreated with the indicated PEDOT:PSS solutions at 75 μg mL^{-1} or PBS only for 10 min at 37 °C. The PEDOT:PSS-treated viral particles were pelleted down through a sucrose gradient centrifugation and ultimately were applied for the infection assay using HEK293T/hACE2 cells. The infectivity of the Spike pseudovirus pretreated with different PEDOT:PSS solutions was (f) visualized by the fluorescence microscope and (g) quantified by flow cytometry. The data are shown as means ± SDs (error bars). Student's *t*-test was used, and $P < 0.05$ indicates a statistically significant difference; $^{**}P < 0.01$, $^{***}P < 0.001$. The scale bar in the figures represents 100 μm.

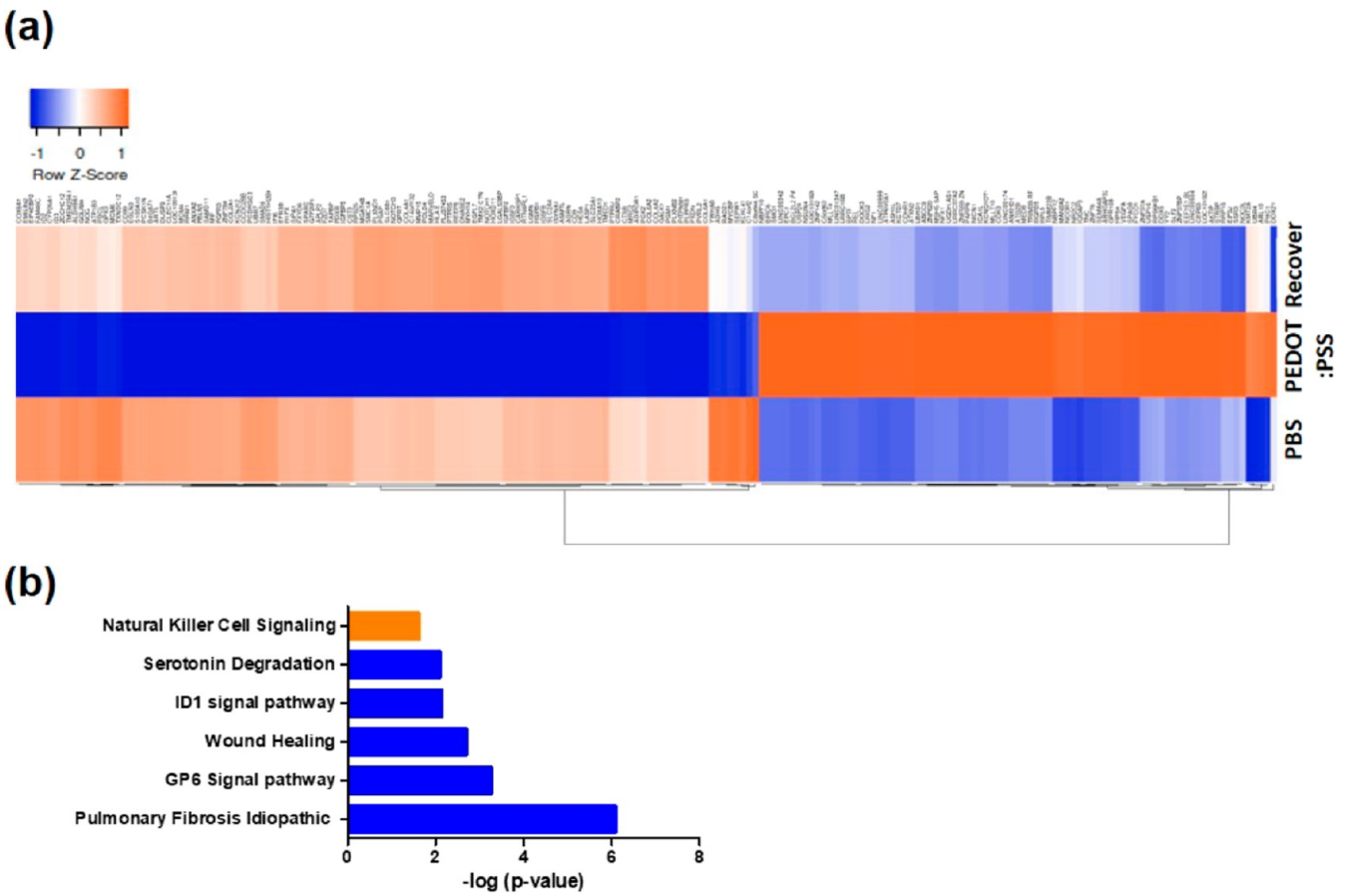

Figure 5. Transcriptome Profiling by Next-Generation Sequencing (NGS) analyses of cells treated with PEDOT:PSS. Here, HEK293T/hACE2 cells were either mock-treated (PBS), treated with PEDOT:PSS at 75 μg mL^{-1} concentration for 24 h (PEDOT:PSS), or treated with PEDOT:PSS at 75 μg mL^{-1} concentration for 24 h and replenished with fresh medium afterward for further 24 h (Recover). RNA extraction was performed and samples were subjected to NGS for transcriptome analysis. The results collected from two independent experiments were analyzed. (a) A heatmap shows the family association among three different groups. Here, the genes showing the translational difference between PBS and PEDOT:PSS groups with a posterior probability of being equally expressed (PPEE) ≤ 0.05 are shown and compared to the recovered group. (b) Top-ranked signal pathways regulated by PEDOT:PSS treatment. Here, we compared the transcriptome data collected from PBS and PEDOT:PSS groups with duplicated sequencing data. Genes with the expressional ratio of PPEE ≤ 0.2 were selected for pathway analysis through IPA software, and the enriched pathways with $-\log p$-value > 1.5) were selected and shown as a bar figure.

were synthesized and examined. Nevertheless, only graphene derivatives with polyglycerol sulfate covered with specific 11 carbon atoms in aliphatic chains (G-PGS-C11) showed a satisfying inhibition effect against SARS-CoV-2 infection by using the concentration without the issues causing cell toxicity.[24] This could be due to the fact that the functionalized graphene platforms with long aliphatic chains could penetrate the plasma membrane of the treated cells, which ultimately leads to cell death. Meanwhile, graphene oxide nanosheets can reduce the SARS-CoV-2 infection through interacting and interfering with SARS-CoV-2 surface proteins and cellular receptors.[28] Herein, we showed that PEDOT:PSS solution can exert almost complete inhibition effect on Spike pseudovirus infection while the concentration in culture medium is equal to or higher than 400-fold dilution (37.5 μg mL^{-1} PEDOT:PSS—original concentration of this material is at average 1.5 wt % in water, corresponding to 15 mg mL^{-1}) but without any observation of cell cytotoxicity even at higher concentrations. By using 3200-fold dilution (44.7 μg mL^{-1}), PEDOT:PSS can still reach 50% of the inhibition rate. Instead of using the live SARS-CoV-2 virus, Spike pseudovirus offers a good platform specifically for monitoring viral binding and entry to the host cells, which are essential steps for a virus to enter the host cells before the initiation of viral replication.[58−62] In consideration of its simple formula, mass production, organic without heavy metals, cheap price, biodegradable feature, and no further demands for the advanced technologies to process, PEDOT:PSS solution

https://doi.org/10.1021/acs.biomac.2c00271
Biomacromolecules XXXX, XXX, XXX−XXX

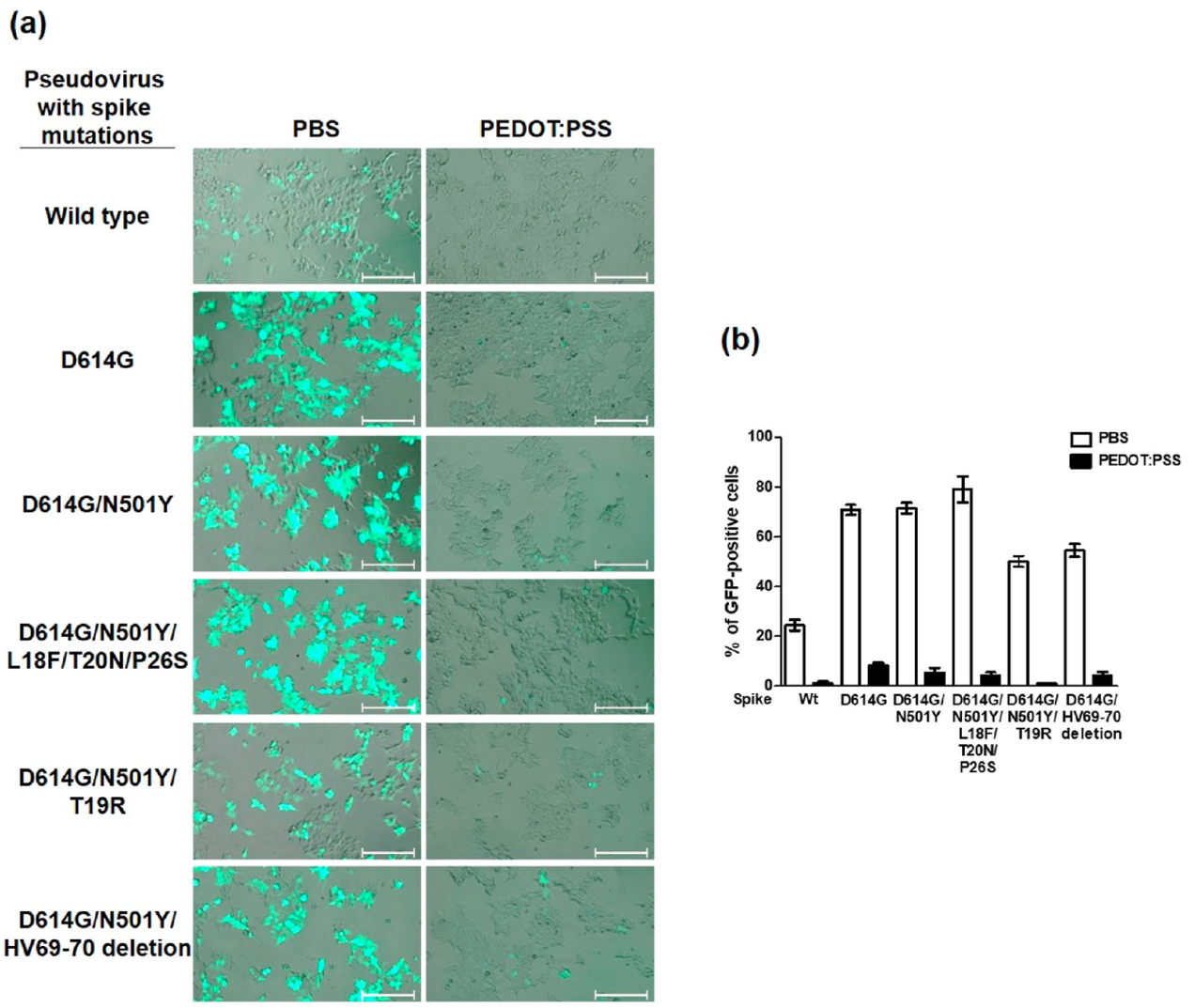

Figure 6. Influence of spike mutations on PEDOT:PSS-mediated downregulation of viral infectivity. Different Spike pseudovirions were produced using a plasmid encoding different spike envelopes together with the lentiviral vector encoding GFP. After the purification of the pseudovirions, their transduction efficiency was evaluated by exposing HEK293T/hACE2 cells to the same amount of viral supernatant with or without the supplement of PEDOT:PSS at 75 μg mL^{-1}. The transduction efficiency of these Spike pseudovirions was visualized by (a) fluorescence microscopy and (b) quantified by flow cytometry 48 h post-infection. The bar figure in (b) shows the mean ± SD (error bars). Unpaired Student's *t*-test was used; ***$P < 0.001$. The scale bar represents 100 μm.

should be considered as a potential material which could be applied in the anti-SARS-CoV-2 field.

Mechanistically, our data showed that PEDOT:PSS can directly inhibit the infectivity of Spike pseudovirus toward ACE2-expressing cells by directly inhibiting the binding ability of the viruses to the cells. However, we noticed that these PEDOT:PSS-treated Spike pseudoviruses can still be successfully pelleted down through a sucrose gradient centrifugation. These results implied that the PEDOT:PSS-treated Spike virions were still intact. Overall, our results suggested that PEDOT:PSS might inhibit the interaction of Spike pseudoviruses with ACE2 by neutralizing the binding sites through the charges of these polymers or directly disrupting the virions. Interestingly, several graphene-based materials also show binding ability against SARS-CoV-2.[24,28] We nevertheless did not consider that PEDOT:PSS could destroy these pseudovirions since the inhibition effect of PEDOT:PSS targeting VSV-G pseudotype virus is minimal.

PEDOT:PSS is a polymer that can be formulated with different compositions with various ratios of PEDOT and PSS as well as different processing procedures that could endow these polymers with numerous characteristics, such as viscosity, solubility, and electric resistivity, depending on the formula.[28] Besides using the commercially available PEDOT:PSS solution (AI 4083, Heraeus Clevios) for the whole of our study, we also tested the PEDOT:PSS solutions made in different formulas. Herein, our results showed that all these PEDOT:PSS solutions exclusively have strong inhibition effects on Spike pseudovirus infection in ACE2-expressing cells. We had also validated that these inhibition effects were the result of PEDOT:PSS function in directly targeting the viral particles. However, we observed that only the PEDOT:PSS solution acquired from Heraeus Clevious has the best solubility with no precipitation could be observed during all experimental procedures. Therefore, we suggest that this formula could be the best one for the future usage in cell-based studies or *in vivo* tests in animal models. Meanwhile,

https://doi.org/10.1021/acs.biomac.2c00271
Biomacromolecules XXXX, XXX, XXX−XXX

whether the antiviral activity is specific to PEDOT:PSS or is a common biologic feature of the other ionomers could also be an interesting future topic. Nevertheless, these ionomers should also have high biocompatibility and low cytotoxicity while applied in human medical usage, so more future tests should be performed. On the other hand, we also observed that PEDOT:PSS can only moderately inhibit the infection of VSV-G pseudotype virus (Figure 4d,e) while using the same concentration of PEDOT:PSS that can nearly entirely inhibit spike pseudovirus infection. Further investigation of the broad-spectrum antiviral ability of PEDOT:PSS by testing against more types of viruses will help us to fully understand how to optimize PEDOT:PSS into an antiviral agent that could be applied for most of human pathogenic viruses.

Interestingly, we did observe that the cells pretreated with PEDOT:PSS were also endowed with a mild ability to inhibit the infection of Spike pseudoviruses. By using transcriptomic analyses *via* comparing the cells after 24 h of PEDOT:PSS treatment and the cells subjected to similar treatment conditions but had an additional 1 day for recovery after the removal of PEDOT:PSS, several interesting gene candidates had been found to be highly upregulated or downregulated post-PEDOT:PSS treatment; this result can be repeated by two independent experiments (Supporting Information Table S2). These data showed that the cells receiving PEDOT:PSS treatment within 24 h altered the signal pathways, including the elevated natural killer cell signaling, and the down-regulation of pulmonary fibrosis idiopathic pathways, both of which have clear benefits in relieving the infection of SARS-CoV-2.[63−65] Meanwhile, four other pathways, including the GP6 signal pathway, wound .healing pathway, ID1 signal pathway, and serotonin degradation pathway, were also downregulated. Interestingly, GP6 signal pathways and ID1 protein expression had been reported to be highly elevated after SARS-CoV-2 infection, while their roles in the pathogenesis of SARS-CoV-2 are still barely understood.[66,67] Meanwhile, the downregulation of serotonin levels in the serum was reported in SARS-CoV-2-infected patients.[68] Indeed, the downregulation of wound healing pathways could reduce the tissue repairing post-viral infection, while some reports indicated that the aberrant wound healing may lead to more severe scarring and fibrosis than other forms of acute respiratory distress syndrome (ARDS).[69] It is very surprising that PEDOT:PSS treatment allows 293T/hACE2 to be endowed with multiple pathway alteration that could benefit the symptoms post-SARS-CoV-2 infection, whereas more detailed mechanisms of PEDOT:PSS on other types of cells should also be carefully investigated before the possible usage *in vivo*. We also validated that most of these gene alterations could be reversed after the removal of PEDOT:PSS for merely 24 h (Figure 5a, Supporting Information Table S2). Indeed, the expression level of some genes had not been entirely reverted back to the original gene expression level after the removal of PEDOT:PSS for 24 h, whereas their expression levels are clearly reverted to the direction similar to the cells without the treatment of PEDOT:PSS, and it might require a longer time to reach similar levels as the untreated cells. Regardless, our results clearly showed that PEDOT:PSS solution could alter the cellular responses through the alternation of RNA transcriptome transiently, which offers many benefits to relieve the symptoms that accompanied after SARS-CoV-2 infection. Moreover, whether this alternation benefits other human diseases or not deserves further investigation on more types of cells and also *in vivo*.

Ultimately, the fast-accumulating mutations of SARS-CoV-2 observed in the current COVID-19 pandemic is a critical issue since many spike protein mutations have led to the escape of the new viral variants from the protection initiated by the vaccines. Therefore, by using Spike pseudoviruses incorporated with the spike protein containing different key mutations, we here could demonstrate that PEDOT:PSS offered broad-spectrum and excellent inhibitory effects against Spike pseudovirus infection, including the currently pandemic causing Delta and Omicron strains that had been reported with strong ability to escape the neutralizing ability derived from the currently available vaccines.[70−72]

5. CONCLUSION

SARS-CoV-2 is a virus that could rapidly evolve and gain mutations causing major challenges for the current drug and vaccine development. PEDOT:PSS is an excellent biomaterial that has advantages of low cell toxicity, biodegradable feature, and low cost. Here, we have additionally demonstrated a new usage of PEDOT:PSS solution in inhibiting SARS-CoV-2 infection through blocking viral binding to the host cells. We found that PEDOT:PSS solution could block more than 90% infection of the Spike pseudovirus to the host cells with broad-spectrum activity. Our results suggest a new therapeutic strategy to prevent SARS-CoV-2 infection by reducing its attachment and entry to the cells that can ultimately impede the spreading of this emerging virus as well as other pathogens that might also be targeted by PEDOT:PSS.

■ ASSOCIATED CONTENT

Supporting Information

The Supporting Information is available free of charge at https://pubs.acs.org/doi/10.1021/acs.biomac.2c00271.

SARS-CoV-2 Spike pseudovirus infecting HEK293T/hACE2 cells with high specificity and oligonucleotides used in the study (PDF)

■ AUTHOR INFORMATION

Corresponding Author

Ming-Han Tsai − *Institute of Microbiology and Immunology, National Yang Ming Chiao Tung University, Taipei City 11221, Taiwan*; orcid.org/0000-0001-5563-3057; Email: m.tsai@nycu.edu.tw

Authors

Jo-Ning Hung − *Institute of Microbiology and Immunology, National Yang Ming Chiao Tung University, Taipei City 11221, Taiwan*

Di Ngoc Kha Vo − *Institute of Microbiology and Immunology, National Yang Ming Chiao Tung University, Taipei City 11221, Taiwan*

Ha Phan Thanh Ho − *Institute of Microbiology and Immunology, National Yang Ming Chiao Tung University, Taipei City 11221, Taiwan*

Complete contact information is available at: https://pubs.acs.org/10.1021/acs.biomac.2c00271

Author Contributions

M.-H.T. designed the study. J.-N.H., D.-N.K.V., H.-P T. H., and M.-H. T performed the experiment. J.-N.H., D.-N.K.V.,

https://doi.org/10.1021/acs.biomac.2c00271
Biomacromolecules XXXX, XXX, XXX−XXX

and M.-H. T. analyzed the data. M.-H. T. and D.-N.K.V. wrote the manuscript. J.-N.H. and D.-N.K.V. contributed equally to this work and their authorships are listed alphabetically.

Notes

The authors declare no competing financial interest.

■ ACKNOWLEDGMENTS

We would like to thank the National RNAi Core Facility at Academia Sinica in Taiwan for providing lentiviral vectors and reagents. We are also grateful to DAILY POLYMER Corporation in Taiwan for providing PEDOT:PSS with different formulas for testing. This work was supported by the Ministry of Science and Technology (MOST) of Taiwan (grant number: MOST 109-2327-B-010-005) and by the Young Scholar Fellowship (Columbus) Program (grant numbers: MOST 110-2636-B-A49-002 and MOST 111-2636-B-A49-003).

■ REFERENCES

(1) WHO, Coronavirus (COVID-19) Dashboard. https://covid19.who.int/ (accessed 2022-June-8th).

(2) Walls, A. C.; Park, Y. J.; Tortorici, M. A.; Wall, A.; McGuire, A. T.; Veesler, D. Structure, Function, and Antigenicity of the SARS-CoV-2 Spike Glycoprotein. *Cell* **2020**, *183*, 1735.

(3) Wrapp, D.; Wang, N.; Corbett, K. S.; Goldsmith, J. A.; Hsieh, C. L.; Abiona, O.; Graham, B. S.; McLellan, J. S. Cryo-EM structure of the 2019-nCoV spike in the prefusion conformation. *Science* **2020**, *367*, 1260−1263.

(4) Tregoning, J. S.; Flight, K. E.; Higham, S. L.; Wang, Z.; Pierce, B. F. Progress of the COVID-19 vaccine effort: viruses, vaccines and variants versus efficacy, effectiveness and escape. *Nat. Rev. Immunol.* **2021**, *21*, 626−636.

(5) Krammer, F. SARS-CoV-2 vaccines in development. *Nature* **2020**, *586*, 516−527.

(6) Li, J.; Lai, S.; Gao, G. F.; Shi, W. The emergence, genomic diversity and global spread of SARS-CoV-2. *Nature* **2021**, *600*, 408−418.

(7) Washington, N. L.; Gangavarapu, K.; Zeller, M.; Bolze, A.; Cirulli, E. T.; Schiabor Barrett, K. M.; Larsen, B. B.; Anderson, C.; White, S.; Cassens, T.; Jacobs, S.; Levan, G.; Nguyen, J.; Ramirez, J. M.; Rivera-Garcia, C.; Sandoval, E.; Wang, X.; Wong, D.; Spencer, E.; Robles-Sikisaka, R.; Kurzban, E.; Hughes, L. D.; Deng, X.; Wang, C.; Servellita, V.; Valentine, H.; De Hoff, P.; Seaver, P.; Sathe, S.; Gietzen, K.; Sickler, B.; Antico, J.; Hoon, K.; Liu, J.; Harding, A.; Bakhtar, O.; Basler, T.; Austin, B.; Isaksson, M.; Febbo, P.; Becker, D.; Laurent, M.; McDonald, E.; Yeo, G. W.; Knight, R.; Laurent, L. C.; de Feo, E.; Worobey, M.; Chiu, C.; Suchard, M. A.; Lu, J. T.; Lee, W.; Andersen, K. G. Genomic epidemiology identifies emergence and rapid transmission of SARS-CoV-2 B.1.1.7 in the United States. *medRxiv.* **2021**, DOI: 10.1101/2021.02.06.21251159, medRxiv Preprint ataccessed 2022-June-8th).

(8) Liu, C.; Ginn, H. M.; Dejnirattisai, W.; Supasa, P.; Wang, B.; Tuekprakhon, A.; Nutalai, R.; Zhou, D.; Mentzer, A. J.; Zhao, Y.; Duyvesteyn, H. M. E.; López-Camacho, C.; Slon-Campos, J.; Walter, T. S.; Skelly, D.; Johnson, S. A.; Ritter, T. G.; Mason, C.; Costa Clemens, S. A.; Gomes Naveca, F.; Nascimento, V.; Nascimento, F.; Fernandes da Costa, C.; Resende, P. C.; Pauvolid-Correa, A.; Siqueira, M. M.; Dold, C.; Temperton, N.; Dong, T.; Pollard, A. J.; Knight, J. C.; Crook, D.; Lambe, T.; Clutterbuck, E.; Bibi, S.; Flaxman, A.; Bittaye, M.; Belij-Rammerstorfer, S.; Gilbert, S. C.; Malik, T.; Carroll, M. W.; Klenerman, P.; Barnes, E.; Dunachie, S. J.; Baillie, V.; Serafin, N.; Ditse, Z.; Da Silva, K.; Paterson, N. G.; Williams, M. A.; Hall, D. R.; Madhi, S.; Nunes, M. C.; Goulder, P.; Fry, E. E.; Mongkolsapaya, J.; Ren, J.; Stuart, D. I.; Screaton, G. R. Reduced neutralization of SARS-CoV-2 B.1.617 by vaccine and convalescent serum. *Cell* **2021**, *184*, 4220−4236.

(9) Kaku, Y.; Kuwata, T.; Zahid, H. M.; Hashiguchi, T.; Noda, T.; Kuramoto, N.; Biswas, S.; Matsumoto, K.; Shimizu, M.; Kawanami, Y.; Shimura, K.; Onishi, C.; Muramoto, Y.; Suzuki, T.; Sasaki, J.; Nagasaki, Y.; Minami, R.; Motozono, C.; Toyoda, M.; Takahashi, H.; Kishi, H.; Fujii, K.; Tatsuke, T.; Ikeda, T.; Maeda, Y.; Ueno, T.; Koyanagi, Y.; Iwagoe, H.; Matsushita, S. Resistance of SARS-CoV-2 variants to neutralization by antibodies induced in convalescent patients with COVID-19. *Cell Rep.* **2021**, *36*, 109385.

(10) Li, Q.; Nie, J.; Wu, J.; Zhang, L.; Ding, R.; Wang, H.; Zhang, Y.; Li, T.; Liu, S.; Zhang, M.; Zhao, C.; Liu, H.; Nie, L.; Qin, H.; Wang, M.; Lu, Q.; Li, X.; Liu, J.; Liang, H.; Shi, Y.; Shen, Y.; Xie, L.; Zhang, L.; Qu, X.; Xu, W.; Huang, W.; Wang, Y. SARS-CoV-2 501Y.V2 variants lack higher infectivity but do have immune escape. *Cell* **2021**, *184*, 2362−2371.

(11) Jackson, C. B.; Farzan, M.; Chen, B.; Choe, H. Mechanisms of SARS-CoV-2 entry into cells. *Nat. Rev. Mol. Cell Biol.* **2022**, *23*, 3−20.

(12) Zhang, Y.; Chen, Y.; Li, Y.; Huang, F.; Luo, B.; Yuan, Y.; Xia, B.; Ma, X.; Yang, T.; Yu, F.; Liu, J.; Liu, B.; Song, Z.; Chen, J.; Yan, S.; Wu, L.; Pan, T.; Zhang, X.; Li, R.; Huang, W.; He, X.; Xiao, F.; Zhang, J.; Zhang, H. The ORF8 protein of SARS-CoV-2 mediates immune evasion through down-regulating MHC-I. *Proc. Natl. Acad. Sci. U. S. A.* **2021**, *118*, No. e2024202118.

(13) Konno, Y.; Kimura, I.; Uriu, K.; Fukushi, M.; Irie, T.; Koyanagi, Y.; Sauter, D.; Gifford, R. J.; Nakagawa, S.; Sato, K. SARS-CoV-2 ORF3b Is a Potent Interferon Antagonist Whose Activity Is Increased by a Naturally Occurring Elongation Variant. *Cell Rep.* **2020**, *32*, 108185.

(14) Yuen, C. K.; Lam, J. Y.; Wong, W. M.; Mak, L. F.; Wang, X.; Chu, H.; Cai, J. P.; Jin, D. Y.; To, K. K.; Chan, J. F.; Yuen, K. Y.; Kok, K. H. SARS-CoV-2 nsp13, nsp14, nsp15 and orf6 function as potent interferon antagonists. *Emerg. Microb. Infect.* **2020**, *9*, 1418−1428.

(15) Wu, J.; Shi, Y.; Pan, X.; Wu, S.; Hou, R.; Zhang, Y.; Zhong, T.; Tang, H.; Du, W.; Wang, L.; Wo, J.; Mu, J.; Qiu, Y.; Yang, K.; Zhang, L. K.; Ye, B. C.; Qi, N. SARS-CoV-2 ORF9b inhibits RIG-I-MAVS antiviral signaling by interrupting K63-linked ubiquitination of NEMO. *Cell Rep.* **2021**, *34*, 108761.

(16) Redondo, N.; Zaldívar-López, S.; Garrido, J. J.; Montoya, M. SARS-CoV-2 Accessory Proteins in Viral Pathogenesis: Knowns and Unknowns. *Front. Immunol.* **2021**, *12*, 708264.

(17) Owen, D. R.; Allerton, C. M. N.; Anderson, A. S.; Aschenbrenner, L.; Avery, M.; Berritt, S.; Boras, B.; Cardin, R. D.; Carlo, A.; Coffman, K. J.; Dantonio, A.; Di, L.; Eng, H.; Ferre, R.; Gajiwala, K. S.; Gibson, S. A.; Greasley, S. E.; Hurst, B. L.; Kadar, E. P.; Kalgutkar, A. S.; Lee, J. C.; Lee, J.; Liu, W.; Mason, S. W.; Noell, S.; Novak, J. J.; Obach, R. S.; Ogilvie, K.; Patel, N. C.; Pettersson, M.; Rai, D. K.; Reese, M. R.; Sammons, M. F.; Sathish, J. G.; Singh, R. S. P.; Steppan, C. M.; Stewart, A. E.; Tuttle, J. B.; Updyke, L.; Verhoest, P. R.; Wei, L.; Yang, Q.; Zhu, Y. An oral SARS-CoV-2 M(pro) inhibitor clinical candidate for the treatment of COVID-19. *Science* **2021**, *374*, 1586−1593.

(18) Chu, C. M.; Cheng, V. C.; Hung, I. F.; Wong, M. M.; Chan, K. H.; Chan, K. S.; Kao, R. Y.; Poon, L. L.; Wong, C. L.; Guan, Y.; Peiris, J. S.; Yuen, K. Y.; Group, H. U. S. S. Role of lopinavir/ritonavir in the treatment of SARS: initial virological and clinical findings. *Thorax* **2004**, *59*, 252−256.

(19) Kabinger, F.; Stiller, C.; Schmitzová, J.; Dienemann, C.; Kokic, G.; Hillen, H. S.; Höbartner, C.; Cramer, P. Mechanism of molnupiravir-induced SARS-CoV-2 mutagenesis. *Nat. Struct. Mol. Biol.* **2021**, *28*, 740−746.

(20) Gordon, C. J.; Tchesnokov, E. P.; Schinazi, R. F.; Götte, M. Molnupiravir promotes SARS-CoV-2 mutagenesis via the RNA template. *J. Biol. Chem.* **2021**, *297*, 100770.

(21) Jayk Bernal, A.; Gomes da Silva, M. M.; Musungaie, D. B.; Kovalchuk, E.; Gonzalez, A.; Delos Reyes, V.; Martín-Quirós, A.; Caraco, Y.; Williams-Diaz, A.; Brown, M. L.; Du, J.; Pedley, A.; Assaid, C.; Strizki, J.; Grobler, J. A.; Shamsuddin, H. H.; Tipping, R.; Wan, H.; Paschke, A.; Butterton, J. R.; Johnson, M. G.; De Anda, C. Molnupiravir for Oral Treatment of Covid-19 in Nonhospitalized Patients. *N. Engl. J. Med.* **2022**, *386*, 509−520.

https://doi.org/10.1021/acs.biomac.2c00271
Biomacromolecules XXXX, XXX, XXX−XXX

(22) Beigel, J. H.; Tomashek, K. M.; Dodd, L. E.; Mehta, A. K.; Zingman, B. S.; Kalil, A. C.; Hohmann, E.; Chu, H. Y.; Luetkemeyer, A.; Kline, S.; Lopez de Castilla, D.; Finberg, R. W.; Dierberg, K.; Tapson, V.; Hsieh, L.; Patterson, T. F.; Paredes, R.; Sweeney, D. A.; Short, W. R.; Touloumi, G.; Lye, D. C.; Ohmagari, N.; Oh, M. D.; Ruiz-Palacios, G. M.; Benfield, T.; Fätkenheuer, G.; Kortepeter, M. G.; Atmar, R. L.; Creech, C. B.; Lundgren, J.; Babiker, A. G.; Pett, S.; Neaton, J. D.; Burgess, T. H.; Bonnett, T.; Green, M.; Makowski, M.; Osinusi, A.; Nayak, S.; Lane, H. C. Remdesivir for the Treatment of Covid-19 - Final Report. *N. Engl. J. Med.* **2020**, *383*, 1813−1826.
(23) Hammond, J.; Leister-Tebbe, H.; Gardner, A.; Abreu, P.; Bao, W.; Wisemandle, W.; Baniecki, M.; Hendrick, V. M.; Damle, B.; Simón-Campos, A.; Pypstra, R.; Rusnak, J. M. Oral Nirmatrelvir for High-Risk, Nonhospitalized Adults with Covid-19. *N. Engl. J. Med.* **2022**, *386*, 1397−1408.
(24) Donskyi, I. S.; Nie, C.; Ludwig, K.; Trimpert, J.; Ahmed, R.; Quaas, E.; Achazi, K.; Radnik, J.; Adeli, M.; Haag, R.; Osterrieder, K. Graphene Sheets with Defined Dual Functionalities for the Strong SARS-CoV-2 Interactions. *Small* **2021**, *17*, No. e2007091.
(25) Zhong, H.; Zhu, Z.; Lin, J.; Cheung, C. F.; Lu, V. L.; Yan, F.; Chan, C. Y.; Li, G. Reusable and Recyclable Graphene Masks with Outstanding Superhydrophobic and Photothermal Performances. *ACS Nano* **2020**, *14*, 6213−6221.
(26) Reina, G.; Iglesias, D.; Samorì, P.; Bianco, A. Graphene: A Disruptive Opportunity for COVID-19 and Future Pandemics? *Adv. Mater.* **2021**, *33*, No. e2007847.
(27) Srivastava, A. K.; Dwivedi, N.; Dhand, C.; Khan, R.; Sathish, N.; Gupta, M. K.; Kumar, R.; Kumar, S. Potential of graphene-based materials to combat COVID-19: properties, perspectives, and prospects. *Mater. Today Chem.* **2020**, *18*, 100385.
(28) Unal, M. A.; Bayrakdar, F.; Nazir, H.; Besbinar, O.; Gurcan, C.; Lozano, N.; Arellano, L. M.; Yalcin, S.; Panatli, O.; Celik, D.; Alkaya, D.; Agan, A.; Fusco, L.; Suzuk Yildiz, S.; Delogu, L. G.; Akcali, K. C.; Kostarelos, K.; Yilmazer, A. Graphene Oxide Nanosheets Interact and Interfere with SARS-CoV-2 Surface Proteins and Cell Receptors to Inhibit Infectivity. *Small* **2021**, *17*, No. e2101483.
(29) Serrano-Aroca, Á.; Takayama, K.; Tuñón-Molina, A.; Seyran, M.; Hassan, S. S.; Pal Choudhury, P.; Uversky, V. N.; Lundstrom, K.; Adadi, P.; Palù, G.; Aljabali, A. A. A.; Chauhan, G.; Kandimalla, R.; Tambuwala, M. M.; Lal, A.; Abd El-Aziz, T. M.; Sherchan, S.; Barh, D.; Redwan, E. M.; Bazan, N. G.; Mishra, Y. K.; Uhal, B. D.; Brufsky, A. Carbon-Based Nanomaterials: Promising Antiviral Agents to Combat COVID-19 in the Microbial-Resistant Era. *ACS Nano* **2021**, *15*, 8069−8086.
(30) Ou, L.; Song, B.; Liang, H.; Liu, J.; Feng, X.; Deng, B.; Sun, T.; Shao, L. Toxicity of graphene-family nanoparticles: a general review of the origins and mechanisms. *Part. Fibre Toxicol.* **2016**, *13*, 57.
(31) Ema, M.; Gamo, M.; Honda, K. A review of toxicity studies on graphene-based nanomaterials in laboratory animals. *Regul. Toxicol. Pharmacol.* **2017**, *85*, 7−24.
(32) Zhang, L.; Ouyang, S.; Zhang, H.; Qiu, M.; Dai, Y.; Wang, S.; Wang, Y.; Ou, J. Graphene oxide induces dose-dependent lung injury in rats by regulating autophagy. *Exp. Ther. Med.* **2021**, *21*, 462.
(33) Fan, X.; Nie, W.; Tsai, H.; Wang, N.; Huang, H.; Cheng, Y.; Wen, R.; Ma, L.; Yan, F.; Xia, Y. PEDOT:PSS for Flexible and Stretchable Electronics: Modifications, Strategies, and Applications. *Adv. Sci.* **2019**, *6*, 1900813.
(34) Ahmad Ruzaidi, D. A.; Mahat, M. M.; Shafiee, S. A.; Mohamed Sofian, Z.; Mohmad Sabere, A. S.; Ramli, R.; Osman, H.; Hamzah, H. H.; Zainal Ariffin, Z.; Sadasivuni, K. K. Advocating Electrically Conductive Scaffolds with Low Immunogenicity for Biomedical Applications: A Review. *Polymers* **2021**, *13*, 3395.
(35) Kayser, L. V.; Lipomi, D. J. Stretchable Conductive Polymers and Composites Based on PEDOT and PEDOT:PSS. *Adv. Mater.* **2019**, *31*, No. e1806133.
(36) Mantione, D.; Del Agua, I.; Sanchez-Sanchez, A.; Mecerreyes, D. Poly(3,4-ethylenedioxythiophene) (PEDOT) Derivatives: Innovative Conductive Polymers for Bioelectronics. *Polymers* **2017**, *9*, 354.
(37) Venkatraman, S.; Hendricks, J.; King, Z. A.; Sereno, A. J.; Richardson-Burns, S.; Martin, D.; Carmena, J. M. In vitro and in vivo evaluation of PEDOT microelectrodes for neural stimulation and recording. *IEEE Trans. Neural Syst. Rehabil. Eng.* **2011**, *19*, 307−316.
(38) Berggren, M.; Głowacki, E. D.; Simon, D. T.; Stavrinidou, E.; Tybrandt, K. In Vivo Organic Bioelectronics for Neuromodulation. *Chem. Rev.* **2022**, *122*, 4826−4846.
(39) Svennersten, K.; Larsson, K. C.; Berggren, M.; Richter-Dahlfors, A. Organic bioelectronics in nanomedicine. *Biochim. Biophys. Acta* **2011**, *1810*, 276−285.
(40) Ko, Y.; Kim, J.; Jeong, H. Y.; Kwon, G.; Kim, D.; Ku, M.; Yang, J.; Yamauchi, Y.; Kim, H. Y.; Lee, C.; You, J. Antibacterial poly (3,4-ethylenedioxythiophene):poly(styrene-sulfonate)/agarose nanocomposite hydrogels with thermo-processability and self-healing. *Carbohydr. Polym.* **2019**, *203*, 26−34.
(41) Feig, V. R.; Tran, H.; Lee, M.; Bao, Z. Mechanically tunable conductive interpenetrating network hydrogels that mimic the elastic moduli of biological tissue. *Nat. Commun.* **2018**, *9*, 2740.
(42) Lu, B.; Yuk, H.; Lin, S.; Jian, N.; Qu, K.; Xu, J.; Zhao, X. Pure PEDOT:PSS hydrogels. *Nat. Commun.* **2019**, *10*, 1043.
(43) Tang, Z.; He, H.; Zhu, L.; Liu, Z.; Yang, J.; Qin, G.; Wu, J.; Tang, Y.; Zhang, D.; Chen, Q.; Zheng, J. A General Protein Unfolding-Chemical Coupling Strategy for Pure Protein Hydrogels with Mechanically Strong and Multifunctional Properties. *Adv. Sci.* **2021**, *9*, No. e2102557.
(44) Zhang, S.; Chen, Y.; Liu, H.; Wang, Z.; Ling, H.; Wang, C.; Ni, J.; Çelebi-Saltik, B.; Wang, X.; Meng, X.; Kim, H. J.; Baidya, A.; Ahadian, S.; Ashammakhi, N.; Dokmeci, M. R.; Travas-Sejdic, J.; Khademhosseini, A. Room-Temperature-Formed PEDOT:PSS Hydrogels Enable Injectable, Soft, and Healable Organic Bioelectronics. *Adv. Mater.* **2020**, *32*, 1904752.
(45) Garcia-Beltran, W. F.; St. Denis, K. J.; Hoelzemer, A.; Lam, E. C.; Nitido, A. D.; Sheehan, M. L.; Berrios, C.; Ofoman, O.; Chang, C. C.; Hauser, B. M.; Feldman, J.; Roederer, A. L.; Gregory, D. J.; Poznansky, M. C.; Schmidt, A. G.; Iafrate, A. J.; Naranbhai, V.; Balazs, A. B. mRNA-based COVID-19 vaccine boosters induce neutralizing immunity against SARS-CoV-2 Omicron variant. *Cell* **2022**, *185*, 457−466.
(46) Bolger, A. M.; Lohse, M.; Usadel, B. Trimmomatic: a flexible trimmer for Illumina sequence data. *Bioinformatics* **2014**, *30*, 2114−2120.
(47) Langmead, B.; Salzberg, S. L. Fast gapped-read alignment with Bowtie 2. *Nat. Methods* **2012**, *9*, 357−359.
(48) Li, B.; Dewey, C. N. RSEM: accurate transcript quantification from RNA-Seq data with or without a reference genome. *BMC Bioinf.* **2011**, *12*, 323.
(49) Babicki, S.; Arndt, D.; Marcu, A.; Liang, Y.; Grant, J. R.; Maciejewski, A.; Wishart, D. S. Heatmapper: web-enabled heat mapping for all. *Nucleic Acids Res.* **2016**, *44*, W147−W153.
(50) Harvey, W. T.; Carabelli, A. M.; Jackson, B.; Gupta, R. K.; Thomson, E. C.; Harrison, E. M.; Ludden, C.; Reeve, R.; Rambaut, A.; Peacock, S. J.; Robertson, D. L. SARS-CoV-2 variants, spike mutations and immune escape. *Nat. Rev. Microbiol.* **2021**, *19*, 409−424.
(51) Zhou, W.; Wang, W. Fast-spreading SARS-CoV-2 variants: challenges to and new design strategies of COVID-19 vaccines. *Signal Transduction Targeted Ther* **2021**, *6*, 226.
(52) Liu, Y.; Yan, L. M.; Wan, L.; Xiang, T. X.; Le, A.; Liu, J. M.; Peiris, M.; Poon, L. L. M.; Zhang, W. Viral dynamics in mild and severe cases of COVID-19. *Lancet Infect. Dis.* **2020**, *20*, 656−657.
(53) Fajnzylber, J.; Regan, J.; Coxen, K.; Corry, H.; Wong, C.; Rosenthal, A.; Worrall, D.; Giguel, F.; Piechocka-Trocha, A.; Atyeo, C.; Fischinger, S.; Chan, A.; Flaherty, K. T.; Hall, K.; Dougan, M.; Ryan, E. T.; Gillespie, E.; Chishti, R.; Li, Y.; Jilg, N.; Hanidziar, D.; Baron, R. M.; Baden, L.; Tsibris, A. M.; Armstrong, K. A.; Kuritzkes, D. R.; Alter, G.; Walker, B. D.; Yu, X.; Li, J. Z. SARS-CoV-2 viral load is associated with increased disease severity and mortality. *Nat. Commun.* **2020**, *11*, 5493.

https://doi.org/10.1021/acs.biomac.2c00271
Biomacromolecules XXXX, XXX, XXX−XXX

(54) Harvey, W. T.; Carabelli, A. M.; Jackson, B.; Gupta, R. K.; Thomson, E. C.; Harrison, E. M.; Ludden, C.; Reeve, R.; Rambaut, A.; Consortium, C.-G. U.; Peacock, S. J.; Robertson, D. L. SARS-CoV-2 variants, spike mutations and immune escape. *Nat. Rev. Microbiol.* **2021**, *19*, 409−424.
(55) Andreano, E.; Piccini, G.; Licastro, D.; Casalino, L.; Johnson, N. V.; Paciello, I.; Dal Monego, S.; Pantano, E.; Manganaro, N.; Manenti, A.; Manna, R.; Casa, E.; Hyseni, I.; Benincasa, L.; Montomoli, E.; Amaro, R. E.; McLellan, J. S.; Rappuoli, R. SARS-CoV-2 escape from a highly neutralizing COVID-19 convalescent plasma. *Proc. Natl. Acad. Sci. U. S. A.* **2021**, *118*, No. e2103154118.
(56) Zhou, D.; Dejnirattisai, W.; Supasa, P.; Liu, C.; Mentzer, A. J.; Ginn, H. M.; Zhao, Y.; Duyvesteyn, H. M. E.; Tuekprakhon, A.; Nutalai, R.; Wang, B.; Paesen, G. C.; Lopez-Camacho, C.; Slon-Campos, J.; Hallis, B.; Coombes, N.; Bewley, K.; Charlton, S.; Walter, T. S.; Skelly, D.; Lumley, S. F.; Dold, C.; Levin, R.; Dong, T.; Pollard, A. J.; Knight, J. C.; Crook, D.; Lambe, T.; Clutterbuck, E.; Bibi, S.; Flaxman, A.; Bittaye, M.; Belij-Rammerstorfer, S.; Gilbert, S.; James, W.; Carroll, M. W.; Klenerman, P.; Barnes, E.; Dunachie, S. J.; Fry, E. E.; Mongkolsapaya, J.; Ren, J.; Stuart, D. I.; Screaton, G. R. Evidence of escape of SARS-CoV-2 variant B.1.351 from natural and vaccine-induced sera. *Cell* **2021**, *184*, 2348−2361 e6.
(57) Tang, Z.; Kong, N.; Zhang, X.; Liu, Y.; Hu, P.; Mou, S.; Liljestrom, P.; Shi, J.; Tan, W.; Kim, J. S.; Cao, Y.; Langer, R.; Leong, K. W.; Farokhzad, O. C.; Tao, W. A materials-science perspective on tackling COVID-19. *Nat. Rev. Mater.* **2020**, *5*, 847−860.
(58) Suprewicz, Ł.; Swoger, M.; Gupta, S.; Piktel, E.; Byfield, F. J.; Iwamoto, D. V.; Germann, D.; Reszeć, J.; Marcińczyk, N.; Carroll, R. J.; Janmey, P. A.; Schwarz, J. M.; Bucki, R.; Patteson, A. E. Extracellular Vimentin as a Target Against SARS-CoV-2 Host Cell Invasion. *Small* **2021**, *18*, No. e2105640.
(59) Shang, J.; Wan, Y.; Luo, C.; Ye, G.; Geng, Q.; Auerbach, A.; Li, F. Cell entry mechanisms of SARS-CoV-2. *Proc. Natl. Acad. Sci. U. S. A.* **2020**, *117*, 11727−11734.
(60) Xia, S.; Liu, M.; Wang, C.; Xu, W.; Lan, Q.; Feng, S.; Qi, F.; Bao, L.; Du, L.; Liu, S.; Qin, C.; Sun, F.; Shi, Z.; Zhu, Y.; Jiang, S.; Lu, L. Inhibition of SARS-CoV-2 (previously 2019-nCoV) infection by a highly potent pan-coronavirus fusion inhibitor targeting its spike protein that harbors a high capacity to mediate membrane fusion. *Cell Res.* **2020**, *30*, 343−355.
(61) Sun, M.; Liu, S.; Song, T.; Chen, F.; Zhang, J.; Huang, J. A.; Wan, S.; Lu, Y.; Chen, H.; Tan, W.; Song, Y.; Yang, C. Spherical Neutralizing Aptamer Inhibits SARS-CoV-2 Infection and Suppresses Mutational Escape. *J. Am. Chem. Soc.* **2021**, *143*, 21541−21548.
(62) Liang, K. H.; Chiang, P. Y.; Ko, S. H.; Chou, Y. C.; Lu, R. M.; Lin, H. T.; Chen, W. Y.; Lin, Y. L.; Tao, M. H.; Jan, J. T.; Wu, H. C. Antibody cocktail effective against variants of SARS-CoV-2. *J. Biomed. Sci.* **2021**, *28*, 80.
(63) Bao, C.; Tao, X.; Cui, W.; Hao, Y.; Zheng, S.; Yi, B.; Pan, T.; Young, K. H.; Qian, W. Natural killer cells associated with SARS-CoV-2 viral RNA shedding, antibody response and mortality in COVID-19 patients. *Exp. Hematol. Oncol.* **2021**, *10*, 5.
(64) Witkowski, M.; Tizian, C.; Ferreira-Gomes, M.; Niemeyer, D.; Jones, T. C.; Heinrich, F.; Frischbutter, S.; Angermair, S.; Hohnstein, T.; Mattiola, I.; Nawrath, P.; McEwen, S.; Zocche, S.; Viviano, E.; Heinz, G. A.; Maurer, M.; Kölsch, U.; Chua, R. L.; Aschman, T.; Meisel, C.; Radke, J.; Sawitzki, B.; Roehmel, J.; Allers, K.; Moos, V.; Schneider, T.; Hanitsch, L.; Mall, M. A.; Conrad, C.; Radbruch, H.; Duerr, C. U.; Trapani, J. A.; Marcenaro, E.; Kallinich, T.; Corman, V. M.; Kurth, F.; Sander, L. E.; Drosten, C.; Treskatsch, S.; Durek, P.; Kruglov, A.; Radbruch, A.; Mashreghi, M. F.; Diefenbach, A. Untimely TGFβ responses in COVID-19 limit antiviral functions of NK cells. *Nature* **2021**, *600*, 295−301.
(65) Wendisch, D.; Dietrich, O.; Mari, T.; von Stillfried, S.; Ibarra, I. L.; Mittermaier, M.; Mache, C.; Chua, R. L.; Knoll, R.; Timm, S.; Brumhard, S.; Krammer, T.; Zauber, H.; Hiller, A. L.; Pascual-Reguant, A.; Mothes, R.; Bülow, R. D.; Schulze, J.; Leipold, A. M.; Djudjaj, S.; Erhard, F.; Geffers, R.; Pott, F.; Kazmierski, J.; Radke, J.; Pergantis, P.; Baßler, K.; Conrad, C.; Aschenbrenner, A. C.; Sawitzki, B.; Landthaler, M.; Wyler, E.; Horst, D.; Hippenstiel, S.; Hocke, A.; Heppner, F. L.; Uhrig, A.; Garcia, C.; Machleidt, F.; Herold, S.; Elezkurtaj, S.; Thibeault, C.; Witzenrath, M.; Cochain, C.; Suttorp, N.; Drosten, C.; Goffinet, C.; Kurth, F.; Schultze, J. L.; Radbruch, H.; Ochs, M.; Eils, R.; Müller-Redetzky, H.; Hauser, A. E.; Luecken, M. D.; Theis, F. J.; Conrad, C.; Wolff, T.; Boor, P.; Selbach, M.; Saliba, A. E.; Sander, L. E. SARS-CoV-2 infection triggers profibrotic macrophage responses and lung fibrosis. *Cell* **2021**, *184*, 6243−6261 e27.
(66) Ng, D. L.; Granados, A. C.; Santos, Y. A.; Servellita, V.; Goldgof, G. M.; Meydan, C.; Sotomayor-Gonzalez, A.; Levine, A. G.; Balcerek, J.; Han, L. M.; Akagi, N.; Truong, K.; Neumann, N. M.; Nguyen, D. N.; Bapat, S. P.; Cheng, J.; Martin, C. S.; Federman, S.; Foox, J.; Gopez, A.; Li, T.; Chan, R.; Chu, C. S.; Wabl, C. A.; Gliwa, A. S.; Reyes, K.; Pan, C. Y.; Guevara, H.; Wadford, D.; Miller, S.; Mason, C. E.; Chiu, C. Y. A diagnostic host response biosignature for COVID-19 from RNA profiling of nasal swabs and blood. *Sci. Adv.* **2021**, *7*, No. eabe5984.
(67) Wang, D.; Wang, D.; Huang, M.; Zheng, X.; Shen, Y.; Fu, B.; Zhao, H.; Chen, X.; Peng, P.; Zhu, Q.; Zhou, Y.; Zhang, J.; Tian, Z.; Guan, W.; Wang, G.; Wei, H. Transcriptomic characteristics and impaired immune function of patients who retest positive for SARS-CoV-2 RNA. *J. Mol. Cell Biol.* **2021**, *13*, 748−759.
(68) Soria-Castro, R.; Meneses-Preza, Y. G.; Rodríguez-López, G. M.; Romero-Ramírez, S.; Sosa-Hernández, V. A.; Cervantes-Díaz, R.; Pérez-Fragoso, A.; Torres-Ruíz, J. J.; Gómez-Martín, D.; Campillo-Navarro, M.; Álvarez-Jiménez, V. D.; Pérez-Tapia, S. M.; Chávez-Blanco, A. D.; Estrada-Parra, S.; Maravillas-Montero, J. L.; Chacón-Salinas, R. Severe COVID-19 is marked by dysregulated serum levels of carboxypeptidase A3 and serotonin. *J. Leukoc. Biol.* **2021**, *110*, 425−431.
(69) Mason, R. J. Pathogenesis of COVID-19 from a cell biology perspective. *Eur. Respir. J.* **2020**, *55*, 2000607.
(70) Cao, Y.; Wang, J.; Jian, F.; Xiao, T.; Song, W.; Yisimayi, A.; Huang, W.; Li, Q.; Wang, P.; An, R.; Wang, J.; Wang, Y.; Niu, X.; Yang, S.; Liang, H.; Sun, H.; Li, T.; Yu, Y.; Cui, Q.; Liu, S.; Yang, X.; Du, S.; Zhang, Z.; Hao, X.; Shao, F.; Jin, R.; Wang, X.; Xiao, J.; Wang, Y.; Xie, X. S. Omicron escapes the majority of existing SARS-CoV-2 neutralizing antibodies. *Nature* **2022**, *602*, 657−663.
(71) Iketani, S.; Liu, L.; Guo, Y.; Liu, L.; Chan, J. F.; Huang, Y.; Wang, M.; Luo, Y.; Yu, J.; Chu, H.; Chik, K. K.; Yuen, T. T.; Yin, M. T.; Sobieszczyk, M. E.; Huang, Y.; Yuen, K. Y.; Wang, H. H.; Sheng, Z.; Ho, D. D. Antibody evasion properties of SARS-CoV-2 Omicron sublineages. *Nature* **2022**, *604*, 553−556.
(72) McCallum, M.; Walls, A. C.; Sprouse, K. R.; Bowen, J. E.; Rosen, L. E.; Dang, H. V.; De Marco, A.; Franko, N.; Tilles, S. W.; Logue, J.; Miranda, M. C.; Ahlrichs, M.; Carter, L.; Snell, G.; Pizzuto, M. S.; Chu, H. Y.; Van Voorhis, W. C.; Corti, D.; Veesler, D. Molecular basis of immune evasion by the Delta and Kappa SARS-CoV-2 variants. *Science* **2021**, *374*, 1621−1626.

https://doi.org/10.1021/acs.biomac.2c00271
Biomacromolecules XXXX, XXX, XXX−XXX